AD-A076 598 JOHNS HOPKINS UNIV BALTIMORE MD DEPT OF EARTH AND PL--ETC F/G 20/4
A NEW THEORY OF TURBULENT FLOW IN A PIPE.(U)
SEP 79 R R LONG
UNCLASSIFIED TR-16-SER-C N00014-75-C-0805
NL

| OF |
AD
A076598

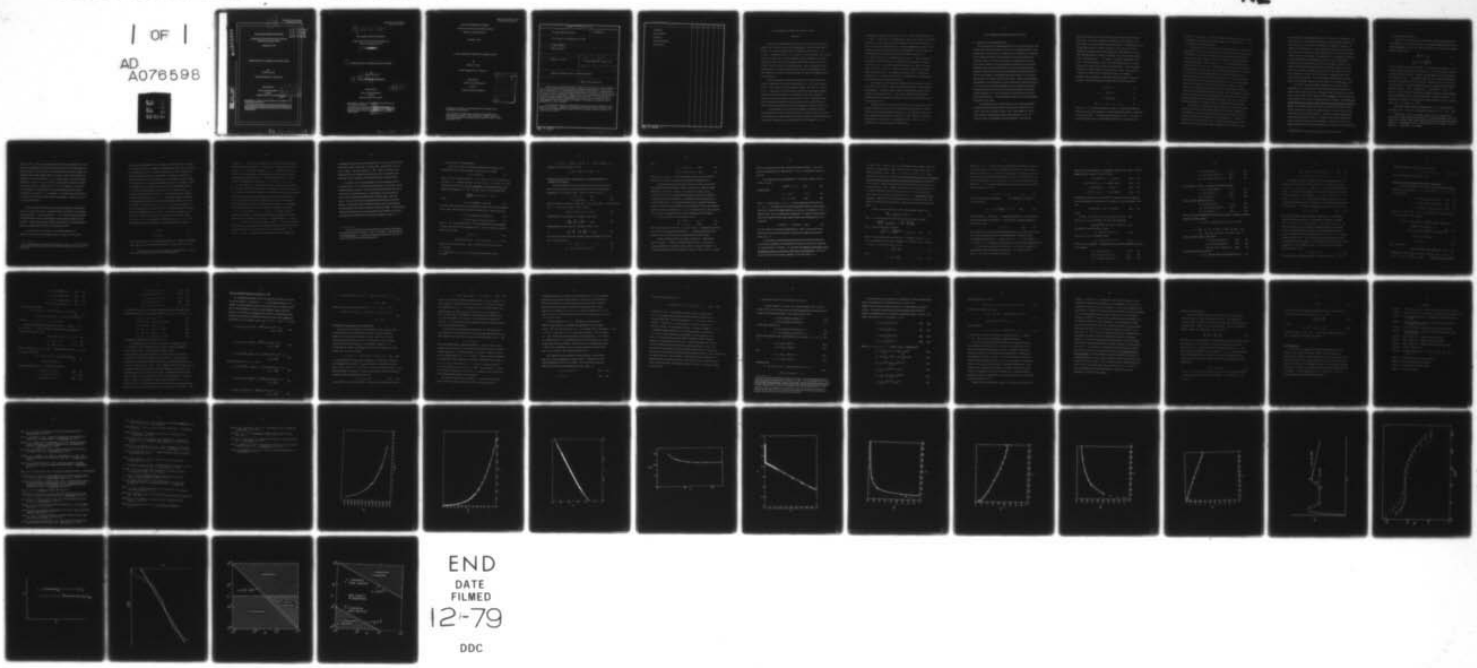

END
DATE
FILMED
12-79
DDC

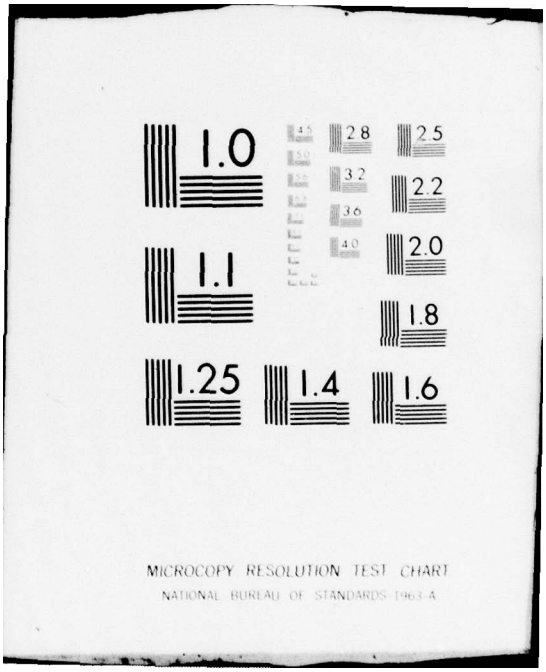
1.0
1.1
1.25
1.4
1.6
1.8
2.0
2.2
2.5
2.8
3.2
3.6
4.0
4.5
5.0
MICROCOPY RESOLUTION TEST CHART
NATIONAL BUREAU OF STANDARDS 1963-A

THE JOHNS HOPKINS UNIVERSITY

Department of Earth and Planetary Sciences
Baltimore, Maryland 21218

September 1979

A NEW THEORY OF TURBULENT FLOW IN A PIPE

By
Robert R. Long

Technical Report No. 16 (Series C)

Sponsored by

Office of Naval Research
and the
National Science Foundation

This research was supported by the Office of Naval Research, Fluid Dynamics Division, under Contract No. N00014-75-C-0805 and the National Science Foundation under Grants No. OCE 76-18887 and ATM76-22284.

(14) TR-16-SER-C

THE JOHNS HOPKINS UNIVERSITY

Department of Earth and Planetary Sciences
Baltimore, Maryland 21218

(11) Sept[redacted]79

(6) A NEW THEORY OF TURBULENT FLOW IN A PIPE

By
(10) Robert R. Long

(9) Technical Report No. 16 (Series C)

(12) 59

Sponsored by

Office of Naval Research
and the
National Science Foundation

(15) This research was supported by the Office of Naval Research, Fluid Dynamics Division, under Contract No. N00014-75-C-0805 and the National Science Foundation under Grants No. GCE 76-18887 and ATM76-22284.

VNSF

406 755

THE JOHNS HOPKINS UNIVERSITY

Department of Earth and Planetary Sciences

Baltimore, Maryland 21218

September 1979

A NEW THEORY OF TURBULENT FLOW IN A PIPE

By

Robert R. Long

Technical Report No. 16 (Series C)

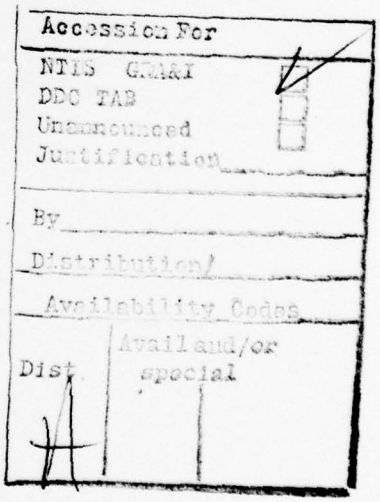

Sponsored by

Office of Naval Research

and the

National Science Foundation

This research was supported by the Office of Naval Research, Fluid Dynamics Division, under Contract No. N00014-75-C-0805 and the National Science Foundation under Grants No. OCE 76-18887 and ATM76-22284.

Security Classification

DOCUMENT CONTROL DATA - R & D

Security classification of title, body of abstract and indexing annotation must be entered when the overall report is classified)

1. ORIGINATING ACTIVITY (Corporate author) The Johns Hopkins University	2a. REPORT SECURITY CLASSIFICATION Unclassifed 2b. GROUP

3. REPORT TITLE

A New Theory of Turbulent Flow in a Pipe

4. DESCRIPTIVE NOTES (*Type of report and inclusive dates*)
Technical Report

5. AUTHOR(S) (*First name, middle initial, last name*)
Robert R. Long

6. REPORT DATE	7a. TOTAL NO. OF PAGES 55	7b. NO. OF REFS 35
8a. CONTRACT OR GRANT NO. N00014-75-C-0805 b. PROJECT NO. c. d.	9a. ORIGINATOR'S REPORT NUMBER(S) Technical Report No. 16(Series C) 9b. OTHER REPORT NO(S) (*Any other numbers that may be assigned this report*)	

10. DISTRIBUTION STATEMENT

Approved for public release. Distribution unlimited

11. SUPPLEMENTARY NOTES	12. SPONSORING MILITARY ACTIVITY Office of Naval Research

13. ABSTRACT

A new theory of turbulent shear flow is based on the discovery of a second boundary layer, which we call the viscous mesolayer, of thickness proportional to Taylor's microscale for the outer flow or, scaling on friction velocity u_τ and viscosity ν, proportional to $R_\tau^{\frac{2}{3}} = (u_\tau a/\nu)^{\frac{2}{3}}$, where a is the outer length. The existence of this layer between the core and the sublayer makes it impossible to match the outer (core) expressions for mean quantities with the inner expressions based on Prandtl's "law of the wall", as in classical theory. Indeed, the supposed region of applicability of the classical theory, namely the layer in which both inner and outer behaviors are imposed, is precisely in the mesolayer where neither behavior may be imposed.

The mesolayer concept is used to develop a new theory of the distribution of mean quantities in pipe flow. Solutions are obtained for the mean quantities in an inertial subrange and in a viscous subrange on either side of the mesolayer. Major alterations in the classical theory result.

DD FORM 1 NOV 65 1473 (PAGE 1)

S/N 0101-807-6801

Security Classification

14 KEY WORDS	LINK A		LINK B		LINK C	
	ROLE	WT	ROLE	WT	ROLE	WT
Turbulence						
Pipe turbulence						
Mesolayer						
Logarithmic theory						
Intermittency						

A NEW THEORY OF TURBULENT FLOW IN A PIPE

ABSTRACT

A new theory of turbulent shear flow is based on the discovery of a second boundary layer, which we call the viscous mesolayer, of thickness proportional to Taylor's microscale for the outer flow or, scaling on friction velocity u_τ and viscosity ν, proportional to $R_\tau^{\frac{1}{2}} = (u_\tau a/\nu)^{\frac{1}{2}}$, where a is the outer length. The existence of this layer between the core and the sublayer makes it impossible to match the outer (core) expressions for mean quantities with the inner expressions based on Prandtl's "law of the wall", as in classical theory. Indeed, the supposed region of applicability of the classical theory, namely the layer in which both inner and outer behaviors are imposed, is precisely in the mesolayer where neither behavior may be imposed.

Each mean quantity is expanded in two infinite series, the first terms of which are appropriate for the outer region which is now $z >> R_\tau^{\frac{1}{2}}$ and for the wall region, $\hat{z} = 0(1)$, where $\hat{z}$ is a new similarity variable, $z/R_\tau^{\frac{1}{2}}$, and z is scaled on u_τ and ν. Equating the two series solves for each of the mean quantities subject to choices of universal constants. It is possible to choose these constants to permit close agreement with the data over most of the flow. Additional evidence for the existence and importance of the mesolayer may be found in the data for pipe flow in which (1) there are two peaks of turbulence energy in the wall region, (corresponding to a first and second component of turbulent motion) as predicted by theory; (2) the rms normal velocity σ_w (dominated in the theory by the first component over a thick region near the wall) is Reynolds-number independent in a layer thick compared to the regions in which the first component of σ_u and

σ_v dominates, as predicted by theory; (3) σ_v and σ_w both reach maxima at or near $z = a_2 R_\tau^{\frac{1}{2}}$, $z = a_3 R_\tau^{\frac{1}{2}}$, and a_2 is considerably less than a_3, all of which are predicted by theory; (4) σ_u (dominated by the first component in a thin layer near the wall) rises to a maximum and then decreases, seemingly approaching a constant. It then begins to increase again (because of the second component). The curve has an inflection point and then another maximum and this inflection point occurs at $z = a_1 R_\tau^{\frac{1}{2}}$ as predicted; (5) the Reynolds stress peaks at $z = a_4 R_\tau^{\frac{1}{2}}$ as predicted; (6) the theory predicts that there is a region just above the sublayer in which $\bar{u}$ increases as $C_0 \ln z$. At a point in the mesolayer there is a change to a smaller slope, $(C_0 + C_{00}) \ln z$ where C_{00} is negative, and this is followed by increasing slopes in the outer region. This complicated pattern is a weak variation about the classical $\kappa^{-1} \ln z$ behavior and, of course, is unattainable in classical theory, but the predicted behavior appears in the data.

Many readers will feel reluctant to abandon the classical theory even in the face of the success of the new theory in predicting the behavior of many measured mean quantities. The paper contains a discussion indicating that the location of the peak of the Reynolds stress at $z \sim R_\tau^{\frac{1}{2}}$ directly contradicts one of the basic assumptions of classical theory regarding the nature of the "buffer layer" between inner and outer layers.

The paper contains a conjecture that the "bursts" are characteristic of the mesolayer and that they grow as they move outward and along the wall. Indeed, if they grow by molecular diffusion, they grow to a size of the order of the mesolayer thickness in the time period of a large core eddy. Finally, an argument is advanced that the intermittency γ is proportional to $R_\tau^{-\frac{1}{4}}$, yielding $\gamma \sim 0.1 - 0.2$, at typical R_τ, in rough agreement with observations.

A NEW THEORY OF TURBULENT FLOW IN A PIPE

1. The Problem of Turbulent Shear Flow.

The classical theory of turbulent shear flow near a surface (Kármán, 1930, Prandtl, 1932, Monin and Yaglom, 1971, Chp. 3) is enduring (despite the clear experimental evidence that it is too simplistic) because nothing more appealing has been offered and because the theoretical mean velocity and the drag coefficient in a pipe seem close to observations. Its predictions for the root-mean-square velocities are not as good and recent efforts have been made by Townsend (1976) and Perry and Abell (1977) to improve the theory for these. Many other efforts have been made to develop higher-order approximations for various mean quantities assuming that the classical theory is a correct first approximation, for example Afzal and Yajnik (1973). Most such investigations, including those of the present paper, lead to mathematical expressions involving one or more universal, unknown constants, and it is usually not convincing to demonstrate agreement with the data over the limited ranges of the theories when the constants are, in fact, chosen to force agreement at one or more points of the data curves. The present paper contains a theory which hopefully passes more severe tests.

A useful approach to the classical theory was developed independently by Izakson (1937) and Millikan (1938) who assumed two regions of flow, an "inner" region near the surface, and an "outer" region further out. In the inner region it is assumed that the outer length parameter a (e.g., the radius of a pipe) is unimportant for all mean quantities. This assump-

tion was first advanced by Prandtl (1925, 1932) and is called the "universal law of the wall". We call this assumption "independence of outer length". In the outer region, it is assumed that the viscosity coefficient ν is unimportant for mean velocity shears and for the velocity defect $(u_o - \bar{u})$ and, indeed, for all mean quantities not connected directly to the small scales of the turbulence. This is called "Reynolds number similarity" (Townsend, 1976) and was also formulated first by von Kármán (1930). We call this assumption "independence of viscosity". Both assumptions have been verified by measurements, for example Fritsch (1928), Laufer (1954), and Perry and Abell (1975). A third assumption is that there is a finite region of overlap of the two regions. We discuss this assumption at length in Section 4 and find it wanting. Nevertheless, using these three assumptions, mathematical operations similar to those used in Section 3 lead to the fundamental results for the overlap region, namely

$$\bar{u} = \frac{1}{\kappa} \ell n\, z + A \tag{1}$$

$$u_o - \bar{u} = -\frac{1}{\kappa} \ell n\, \zeta + B \tag{2}$$

$$u_o = \frac{1}{\kappa} \ell n\, R_\tau + A + B \tag{3}$$

$$-\overline{uw} = 1, \quad \sigma_u = A_1, \quad \sigma_v = A_2, \quad \sigma_w = A_3 \tag{4}$$

where σ_u, σ_v, σ_w are root-mean-square velocities, ζ is distance from the wall, scaled on a, and all other quantities are scaled on the inner variables ν and friction velocity at the wall u_τ. The Reynolds number used here is $u_\tau a/\nu = R_\tau$ and u_o is the non-dimensional outer velocity which, for pipe flow, is the velocity at the

centerline. The constant κ is called von Kármán's constant and, except for one set of measurements (Businger, et al., 1971), appears to be about the same, $\kappa \cong 0.41$, in all laboratory and geophysical flows.

The agreement of (1)-(3) with the data is puzzling because close observation of phenomena in shear flow over the past 15-20 years indicates that the structure of the turbulence is very different from the picture inherent in the classical theory. To be specific, all the results in (1)-(4) may be obtained by dimensional analysis assuming independence of both ν and a in $1 << z << R$, and this approach predicts further that all length scales in the overlap region are of the order of the distance z from the surface. Measurements, however, (Mitchell and Hanratty, 1966, Tritton, 1967) indicate that the longitudinal length scale is much larger than z near the surface and may be of the order of the outer length scale a. We know for certain now that large eddies, associated with motions in the core, are exerting a strong influence in the region just above and even in the viscous sublayer. Another example is the appearance of the "bursts" above the viscous sublayer which have a time period much longer than the only time period of the classical theory, namely distance from the surface divided by friction velocity, and which seems to scale on the outer variables (Laufer and Narayanan, 1971, Rao, et al., 1971). Obviously, then the independence of a assumed in the so-called buffer region is untenable.

The existence and importance of large eddies near a wall have been demonstrated by theoretical and experimental studies of the distortion of turbulence in a wind tunnel by a surface parallel to the flow and moving at the speed of the free stream to yield shear-free turbulence (Uzkan and Reynolds, 1967, Thomas and Hancock, 1977, Hunt and Graham, 1978). At least in the initial stages of the distortion (near the leading edge),the horizontal dimensions of the eddies just above

the viscous layer are proportional to the size of the eddies in the mainstream. The author (Long, 1978) has discussed the importance of this distortion in problems of the mixed layer in stratified fluids in laboratory and geophysical situations. In problems of shear flow there is a large production of eddy energy near the surface but surely the large eddies of the outer region must "feel" the wall in ways similar to those of shear-free turbulence. Townsend (1976, p. 161) regards the turbulence as being composed of two components, one called a "wall" component whose dimensions scale with distance from the wall, and the other an "inactive" component with horizontal dimensions of the order of the outer length, and vertical dimensions of the order of distance from the wall. Perry and Abell (1977) call these components "universal" and "non-universal", respectively, and we will adopt this latter terminology. The two components of motion appear clearly in spectra at high Reynolds numbers (Perry and Abell, 1975, Bullock, et al., 1978).

The theory in this paper employs independence of a near the wall and independence of ν far from the wall in the first approximations so that there are still the sublayer and the outer layer. It appears, however, that there is a second, thicker viscous boundary layer, which we call the mesolayer, whose existence must be fundamental for the problem of turbulent shear flow in general, and that this layer, intruding between inner and outer layers, prevents the overlap assumed in classical theory.[1] The mesolayer appears to be the layer in which the horizontal velocity of the large eddies of the non-universal motion reduces to zero at the wall as in the experiments of Uzkan and Reynolds (1967). Indeed, we find that its thickness, as determined theoretically in Section 2, is identical to the empirical thickness $R_\tau^{\frac{1}{2}}$ of the viscous layer found by Uzkan and Reynolds. The layer is similar also in character and behavior to the laminar boundary layer in flow above an oscillating plane.

[1] The failure of the classical approach is shown in detail in Section 4.

2. Discussion of the Mesolayer.

In Section 1, we presented some general ideas about turbulent shearing flow. To be definite, we now confine attention to a smooth pipe although the ideas have very general applicability. We may write down the two non-trivial, exact, mean equations of motion (Laufer, 1954),

$$\frac{d\bar{u}}{dz} - \overline{uw} = 1 - \frac{z}{R_\tau} \tag{5}$$

$$\frac{d}{dz}\left(\bar{p} + \overline{ww}\right) = \frac{\overline{ww} - \overline{vv}}{R_\tau(1-\zeta)} \tag{6}$$

where z is distance from the wall, so that $z = R_\tau$ at the center of the pipe, $\zeta = z/R_\tau$, $\bar{p}$ is the mean pressure and the velocities are u, v, w in the streamwise, transverse and radial (inward) directions. As in the rest of the paper, we scale, generally, on inner variables ν and u_τ. The Reynolds stress $-\overline{uw}$ is zero at the wall and its first derivative with respect to z is zero at the wall. Moreover, $-\overline{uw}$ is zero at the axis of the pipe so that, as measurements also show, it is a maximum at some distance from the wall, say $z = m(R_\tau)$. Therefore, $\bar{u}_{zz} = -1/R_\tau$ both at $z = 0$ and $z = m$. When R_τ is large, the effect of viscosity is confined to a thin layer and the Reynolds stress and the total stress $(1-z/R_\tau)$ are nearly equal, except at very small z. Consequently, the maximum of $-\overline{uw}$ must become closer and closer to 1 as R_τ increases. Thus, near $z = m$, we have[1] $\bar{u}_z \sim m/R_\tau$.

Let us now make the tentative assumption that $\bar{u}_z \sim m^{-1}$ in the region of the maximum of $-\overline{uw}$. The two order-of-magnitude estimates, $\bar{u}_z \sim m^{-1}$ and $\bar{u}_z \sim m/R_\tau$

---

[1] We say $A(R_\tau) \sim B(R_\tau)$ if A/B tends to a finite, non-zero constant as $R_\tau \to \infty$. We also use $A = 0(B)$ to indicate that A/B tends to a constant (independent of R_τ) which may be zero. A point z whose distance from the wall varies from experiment to experiment (i.e., is some function of R_τ) is said to lie always in the mesolayer if, for all large R_τ, $z = \alpha m(R_\tau)$ where α is a constant.

lead to $m \sim R_\tau^{\frac{1}{2}}$. We have an indication in this result of a new boundary layer over which certain quantities change from their universal wall values to those typical of the outer region.[1] This second layer is much thicker than the viscous sublayer over which the mean velocity changes rapidly. It is quite evident in observations, for example, by Laufer (1954, his Fig. 8). If, for the moment, we use the empirical fact that $\bar{u}_{zz}$ is very close to $1/\kappa z^2$ where κ is von Kármán's constant, we predict the maxima of $-\overline{uw}$ at $z = a_4 R_\tau^{\frac{1}{2}}$ where $a_4 = (\kappa)^{-\frac{1}{2}}$, or at values of ζ of 0.016 and 0.047 for Laufer's two experiments in very close agreement with his Figure 8. In contrast, the maximum of σ_u, for example, is very much closer to the wall and is just outside of (fixed with respect to) the viscous sublayer (Laufer's Fig. 25) as we discuss further below.

Perry and Abell (1975) found a layer (in inner variables) in which the data curves of σ_u tend to become level, indicating in their view that the classical theory correctly predicts σ_u = const in a region $1 \ll z \ll R_\tau$. From our present viewpoint the inflection point of the σ_u-profile found in all measurements should lie in the mesolayer. Indeed, these points are further out from the wall at higher Reynolds numbers in rough proportion to $R_\tau^{\frac{1}{2}}$ as we will also see below.

As we have discussed in Section 1, the mesolayer appears to be similar to that in shear-free turbulent flow above a surface, as in the experi-

---

[1] The classical approach also predicts a maximum of $-\overline{uw}$ at $z \sim R_\tau^{\frac{1}{2}}$ but, in ignoring the physical effects of the mesolayer, it fails in other fundamental ways as we see in Section 4.

ment of Uzkan and Reynolds (1967) or, perhaps, in turbulent flow near a surface at some distance from an oscillating grid (Hopfinger and Toly, 1976) as suggested by the author (Long, 1978). The present situation is not a direct analogy to the shear-free problem, however, because there is already one viscous layer at the wall of the pipe and it is not obvious how to obtain another one from a single set of equations. We may obtain both as follows, however: we imagine an initial-value problem of a very long pipe immersed in a Navier-Stokes fluid initially at rest with a suddenly imposed force along it at $t = 0$ creating a stress u_τ^2 on the walls which is then held fixed in time. The pipe will move and eventually come up to a constant speed $u_{0d}(a, \nu, u_\tau)$. We assume complete determinism[1] of the turbulent motion such that the velocity component u_d relative to the wall, for example, is the same at $(x_d, y_d, z_d, t_d ; a, \nu, u_\tau)$ in any two experiments if the initial conditions are identical even after a very long time when the problem becomes statistically steady. At a fixed z, as the radius of the pipe a goes to infinity, we assume that the effect of a becomes weaker and weaker so that $u_d(x_d, y_d, z_d, t_d ; a, \nu, u_\tau)$ approaches a function $u_{1d}(x_d, y_d, z_d, t_d ; \nu, u_\tau)$. The assumption that the limiting function u_{1d} exists means that we may express

$$u = u_1 + u_2 \tag{7}$$

$$\overline{u} = \overline{u}_1 + \overline{u}_2 \tag{8}$$

where we have gone over to non-dimensional notation. u_1 and $\overline{u}_1$ are independent of R_τ and, as we have constructed the problem, u_2 and $\overline{u}_2$ tend to zero as $R_\tau \to \infty$

[1] The reader who is accustomed to thinking of turbulent flow as "random" may read an amplified discussion in Chern and Long (1980).

by letting $a \to \infty$. Then, if we substitute into the set of Navier-Stokes equations, which we denote as N_∞ and let $R_\tau \to \infty$, we obtain a set of equations N_1 involving only u_1, v_1, w_1, p_1 and inner variables, x, y, z, t. The form is the same as for flow over an infinite plane in the infinite half-space above with the constant (dimensional) momentum transfer, u_τ^2, and above the sublayer (e.g., in the mesolayer) independence of ν leads to $\bar{u}_1 = \kappa^{-1} \ln z + A$, $\sigma_{u_1} = A_1$, $\sigma_{v_1} = A_2$, $\sigma_{w_1} = A_3$, etc. where A, A_i are universal constants. Since N_1 does not involve R_τ, it is valid for all R_τ and, therefore, we may subtract N_1 from N to obtain a new set of equations valid for all R_τ, namely N_2. Obviously the non-universal component of motion may be identified with the large-scale motions associated with the core. If we integrate the equation of continuity over a "box" in the mesolayer of vertical dimensions of order m and horizontal dimensions L_x, corresponding to the peak of the energy spectrum as a function of streamwise wave number $k_x = L_x^{-1}$, we get rms values $\sigma_{u_2} \sim \sigma_{v_2} \sim \sigma_{w_2} L_x m^{-1}$. According to our basic concept of the mesolayer, the horizontal eddy velocity of the large eddies is the same order in the mesolayer as in the core. Using independence of ν, we have $\sigma_{u_2} \sim \sigma_{v_2} \sim 1$ in the core and in the mesolayer so that $\sigma_{w_2} \sim m L_x^{-1}$ in the mesolayer. In the shear-free experiments, the horizontal eddy dimensions in the viscous layer are the same order as in the region outside. We assume then that $L_x \sim R_\tau$ so that $\sigma_{w_2} \sim m R_\tau^{-1}$. The thickness of the mesolayer may now be obtained by

integrating the streamwise momentum equation in N_2 twice over the "box" and equating the largest viscous term, of order $\sigma_{u2} R_\tau^4$, to the inertial term[1] of order $\sigma_{u2}^2 R_\tau^3 m^3$. We find a thickness $m = R_\tau^{\frac{1}{2}}$. Thus, we obtain the same expression $R_\tau^{\frac{1}{2}}$ for the boundary-layer thickness and we have identified the mesolayer with the "sloshing" of the large-scale eddies along the surface.

The analysis in this section depends on the two assumptions for the mesolayer that $\bar{u}_z \sim m^{-1}$ and that the axial length scale is of order R_τ for the second component of motion. The first will be discussed further in Section 3. The second, as mentioned earlier, is in accordance with observations by Tritton (1967), Mitchell and Hanratty (1966), Bullock, et al., (1978) and others. These measurements are especially noteworthy because they show that over a considerable range of Reynolds numbers the horizontal length is not only large near the wall but scales best on the outer length. The observations of Mitchell and Hanratty were made remarkably deep within the viscous layer indicating that the large eddies are exerting an influence even for $z < 1$!

---

[1] We use a coordinate system moving at the mean speed of the fluid at the center of the box and assume $\bar{u}_z = 0(z^{-1})$ in the layer. This assumption is verified a posteriori. The argument involving the integrals over the "box" is given in more detail in Chern and Long (1980).

3. The New Theory for Mean Quantities.

Let us now construct a new theory incorporating the mesolayer as a fundamental element. Quite generally, we may write, for example,

$$\bar{u} = \bar{u}_+(z) + \bar{u}_*(\hat{z}, R_\tau) \tag{9}$$

where $\hat{z}$ is a new similarity variable $\hat{z} = z/m$, where $m = R_\tau^{\frac{1}{2}}$ is the thickness of the mesolayer.[1] If $\hat{z}$ = constant, the point z is in the mesolayer. We assume, as a fundamental property of the layer, that <u>all mean quantities are of the same order at all points of the mesolayer,</u> e.g., $\bar{u} - \bar{u}_+ = \bar{u}_*(\hat{z}, R_\tau)$. Then, for some function $h_0(R_\tau)$

$$\frac{\bar{u}_*(\hat{z}, R_\tau)}{h_0(R_\tau)} \to \bar{u}_{*0}(\hat{z}) \text{ as } R_\tau \to \infty, \ \hat{z} \text{ fixed}$$

so that

$$\bar{u} = \bar{u}_+(z) + h_0(R_\tau)\bar{u}_{*0}(\hat{z}) + \bar{u}_{*1}(\hat{z}, R_\tau) \tag{10}$$

where $\overline{u_{*1}}$ in the mesolayer is small compared to $h_0(R_\tau)\bar{u}_{*0}(\hat{z})$. The same argument for $\overline{u_{*1}}$ shows that it must also be of the form $h_1(R_\tau)\bar{u}_{*1}(\hat{z})$. Thus we may write

$$\bar{u} = \bar{u}_+(z) + h_0(R_\tau)\bar{u}_{*0}(\hat{z}) + h_1(R_\tau)\bar{u}_{*1}(\hat{z}) + \dots \tag{11}$$

$$T = T_+(z) + h_{s0}(R_\tau)T_{*0}(\hat{z}) + h_{s1}(R_\tau)T_{*1}(\hat{z}) + \dots \tag{12}$$

where $T = -\overline{uw}$ is the Reynolds stress. The assumption that the first component of motion is the only surviving component as $R_\tau \to \infty$ at fixed z yields two equations in place of (5), namely

$$\bar{u}_+' + T_+ = 1 \tag{13}$$

$$h_0 R_\tau^{-\frac{1}{2}}\bar{u}_{*0}' + h_1 R_\tau^{-\frac{1}{2}}\bar{u}_{*1}' + \dots + h_{s0}T_{*0} + h_{s1}T_{*1} + \dots = -\zeta \tag{14}$$

where primes denote derivatives. Since T and its first derivative are zero at $z = 0$, we have

---

[1] In Section 4, we derive $m \sim R_\tau^{\frac{1}{2}}$ by arguments independent of those of Section 2.

$$h_0 = 1, \bar{u}''_{*0}(0) = -1, \bar{u}_{*1}(0) = 0, \bar{u}''_{*2}(0) = 0, \ldots, \bar{u}'_{*1}(0) = 0, \bar{u}'_{*2}(0) = 0, \ldots$$

Evaluating (14) in the mesolayer, we find

$$h_{s0} = R_\tau^{-\frac{1}{2}}, \; h_1 R_\tau^{-\frac{1}{2}} = h_{s1}, \; h_2 R_\tau^{-\frac{1}{2}} = h_{s2}, \ldots$$

Solutions for Mean Velocities, Reynolds Stress, Dissipation Function and Energy Flux-Divergence.

Let us now match the first approximation for the form for the velocity-defect in the region near the wall with its form in the outer region assuming independence of ν in the outer region. We have, to the present order,

$$u_0 - \bar{u} = \varphi(\zeta) \qquad (M_0) \tag{15}$$

$$\bar{u} = \bar{u}_+(z) + \bar{u}_{*0}(\hat{z}) \qquad (M_1) \tag{16}$$

where we denote here and below regions $(0 \leq z \ll R_\tau)$ by M_1, $(R_\tau^{\frac{1}{2}} \ll z \leq R_\tau)$ by M_0 and $(R_\tau^{\frac{1}{2}} \ll z \ll R_\tau)$ by M_{10}. Using $u_0 = u_0(R_\tau)$, we have

$$u_0(R_\tau) - \bar{u}_+(z) - \bar{u}_{*0}(\hat{z}) = \varphi(\zeta) \quad (M_{10}) \tag{17}$$

Differentiating (17) with respect to R_τ, holding ζ fixed, we get

$$R_\tau \frac{du_0}{dR_\tau} - z \frac{d\bar{u}_+}{dz} - \frac{1}{2} \hat{z} \frac{d\bar{u}_{*0}}{d\hat{z}} = 0 \quad (M_{10}) \tag{18}$$

Differentiating (18) with respect to z, holding R_τ fixed, we get

$$-z \frac{d}{dz} z \frac{d\bar{u}_+}{dz} - \frac{\hat{z}}{2} \frac{d}{d\hat{z}} \hat{z} \frac{d\bar{u}_{*0}}{d\hat{z}} = 0 \quad (M_{10}) \tag{19}$$

The terms in (19) must each equal a constant so that the solutions for $\bar{u}_+$ and u_0 are, to the present order,

$$\bar{u}_+ = C_0 \ell n \, z + C_+ \qquad (z \gg 1) \tag{20}$$

$$u_0 = A_{12} + C_+ + C_* + (C_0 + \tfrac{1}{2} C_{00}) \ell n \, R_\tau \tag{21}$$

Also

$$\bar{u}_{*0} = C_{00} \ell n\, \hat{z} + C_* \qquad (M_{10}) \tag{22}$$

$$u_0 - \bar{u} = A_{12} - (C_0 + C_{00}) \ell n\, \zeta \qquad (M_{10}) \tag{23}$$

where $C_0, C_+, A_{12}, C_*, C_{00}$ are universal constants and we reject a solution of the form $z^{-1} \ell n\, z$ for $d\bar{u}_+/dz$ because of the principle of independence of ν.

The expression in (20) for the mean velocity is the same as in classical theory although they have different regions in which they are supposed to apply. Obviously, C_0 is close to κ^{-1} where κ is von Kármán's constant. The C_{00}-terms in (21) and (23) are absent in classical theory, but we have no reason for assuming this in the present analysis, even though experiment indicates that C_{00} is small compared to C_0. The fact that the profile of $\bar{u}$ is logarithmic both below and above the center of the mesolayer with the contribution of the second component small means that $\bar{u}$ (as opposed to $\sigma_u, \sigma_v, \sigma_w$, as we discuss below) is a poor indicator of the mesolayer and explains why the classical theory has been so enduring.

If we use (20) and (22) in (13) and (14), we find

$$T_+ = 1 - C_0 z^{-1} \qquad (z \gg 1) \tag{24}$$

$$T_{*0} = -\hat{z} - C_{00} \hat{z}^{-1} \qquad (M_{10}) \tag{25}$$

Notice that the equation $T_+' + R_\tau^{-1} T_{*0}' = 0$, or $C_0 \hat{z}^{-2} + T_{*0}'(\hat{z}) = 0$, defining the position of the maximum of the Reynolds stress, yields $\hat{z} = a_+$, showing that the peak of the Reynolds stress is in the mesolayer as suggested above and by the data.

A physical interpretation of our results is that $d\bar{u}_+/dz$ represents the shear in a region $z \gg 1$ above an infinite flat plate and since a is absent and viscosity should become negligible, $z d\bar{u}_+/dz$ must be a universal constant C_0 on dimensional grounds in agreement with (20). When R_τ is finite, $z d\bar{u}/dz = C_0$ should

hold in some region near the wall. On the other hand in $M_{10}(R_\tau^{\frac{1}{2}} \ll z \ll R_\tau)$ both ν and a are unimportant and we again find $z\bar{u}_z = C_0 + C_{00}$ is a constant in agreement with (23).

Let us now assume strict independence of ν in the outer region to solve for T in M_{10}. We have

$$T_+ + R_\tau^{-\frac{1}{2}} T_{*0} = \chi_0(\zeta) \qquad (M_{10}) \qquad (26)$$

Matching yields

$$T_+ = \kappa_1 - \kappa_2 z^{-1} \qquad (z \gg 1) \qquad (27)$$

$$T_{*0} = \kappa_3 \hat{z} + \kappa_2 \hat{z}^{-1} \qquad (M_{10}) \qquad (28)$$

Since $\chi = 1-\zeta$ to this order, $\kappa_1 = 1$, $\kappa_3 = -1$ and by comparison with (24) and (25), $\kappa_2 = -C_{00} = C_0$. According to (23) we lose the logarithmic behavior for the velocity defect in M_{10}. This seems highly unlikely but, in any case, the deduction, $C_0 + C_{00} = 0$, cannot be made once we recognize that independence of ν cannot be strictly correct. Thus we are required to add a higher approximation on the right-hand side of (26) of the form

$$T_+ + R_\tau^{-\frac{1}{2}} T_{*0} = 1 - \zeta + R_\tau^{-1} \chi_1(\zeta) \qquad (M_{10}) \qquad (29)$$

If we now match, we find that the coefficients of z^{-1} and $\hat{z}^{-1}$ in (27) and (28) need not be the same and we get the behavior of (24) and (25) without the requirement that $C_0 + C_{00} = 0$.

We may make two interesting interpretations of the mesolayer which help to overcome the difficulty in understanding how molecular friction can be important in a region far above the sublayer. We may define the sublayer as the region in which the Reynolds stresses are of the same order as the viscous stresses. In the mesolayer the viscous stress becomes negligible, as we would expect, i.e.,

$\bar{u}_z / -(\overline{u'w'}) \to R_\tau^{-\frac{1}{2}}$. However, $-\overline{u'w'}$ is nearly constant in the mesolayer (indeed the classical logarithmic layer is often referred to as the "constant stress" layer) so that its derivative is small: $(-\overline{u'w'})_z \sim z^{-2} + R_\tau^{-1} T'_{*0}$ or $(-\overline{u'w'})_z \sim R_\tau^{-1}$. This is exactly of the order of $\bar{u}_{zz}$ revealing that in the mesolayer the forces due to the Reynolds stress are of the same order as the forces due to the viscous stresses and that both are very small. Another interpretation of the viscous effects in the mesolayer is to conjecture that the "bursts" originate in the region very near the wall and then grow by molecular diffusion, with dimensions of order $(\nu t)^{\frac{1}{2}}$. In a time period of the order of the large core eddies this becomes $(H\nu/u_\tau)^{\frac{1}{2}}$, i.e., of the thickness of the mesolayer. Apparently the bursts transport most of the momentum and the small change with height of the momentum flux is controlled by the viscous growth of these bursts.

Further discussion requires use of the energy equation (Laufer, 1954):

$$T \frac{d\bar{u}}{dz} + \frac{1}{(1-zR_\tau^{-1})} \frac{\partial}{\partial z} [(1-zR_\tau^{-1})F] = \epsilon \tag{30}$$

where ϵ is the dissipation function non-dimensionalized by inner variables,

$$\epsilon = \overline{\frac{\partial u'_i}{\partial x_j} \frac{\partial u'_i}{\partial x_j}} + \frac{1}{R_\tau (1-zR_\tau^{-1})} \left(4\overline{v' \frac{\partial w'}{\partial y}} + \frac{\overline{v'^2 + w'^2}}{R_\tau (1-zR_\tau^{-1})} \right)$$

and F is the non-dimensional energy flux

$$\nu \frac{\partial \overline{(q'^2/2)}}{\partial z} + \frac{-\overline{w'(P' + q'^2/2)}}{u_\tau^3} = F = F_+ + h_{\epsilon 0} F_{*0} \qquad (M_1) \tag{31}$$

where P' is the turbulence pressure function, q' is turbulence speed, u', v', w' or u'_i are turbulence velocities and all quantities are scaled on u_τ and ν. Writing $\epsilon = \epsilon_+ + h_{\epsilon 0} \epsilon_{*0}$, in (M_1) and using Eq. (24) and

$$\epsilon_+ = T_+ \frac{d\bar{u}_+}{dz} + \frac{dF_+}{dz} \tag{32}$$

we get

$$\epsilon_+ = C_0 z^{-1} + \frac{dF_+}{dz} \qquad (z \gg 1) \tag{33}$$

Suppose $dF_+/dz \sim z^{-1}$. Then F_+ behaves logarithmically and therefore, because all correlation coefficients for the first component of motion must, to first order, be universal constants for $z \gg 1$, velocities in the mesolayer are of larger order than one, contrary to our fundamental assumption in deriving $m \sim R_\tau^{\frac{1}{2}}$ from the N_2-set of Navier-Stokes equations. Also, of course, $F_+ \sim \ell n\, z$ violates the principle of independence of ν. We reject this logarithmic behavior and require that F_+ be smaller. Then it follows from (33) that

$$\epsilon_+ = C_0 z^{-1}, \quad F_+ = D_0 \qquad (z \gg 1) \qquad (34)$$

where D_0 is a new universal constant. If we subtract (32) from (30), we get, to first order,

$$h_{\nu 0}\epsilon_{*0} = h_{\epsilon 0} R_\tau^{-\frac{1}{2}} \frac{dF_{*0}}{d\hat{z}} + C_{00}\hat{z}^{-1}R_\tau^{-\frac{1}{2}} \qquad (M_{10}) \qquad (35)$$

This shows that $h_{\nu 0} = R_\tau^{-\frac{1}{2}}$ and $h_{\epsilon 0} = 1$. Applying independence of ν to F in the outer region and matching, we find that F_{*0} is constant in M_{10}. Equating coefficients of $R_\tau^{-\frac{1}{2}}$ in (35), we find

$$\epsilon_{*0} = C_{00}\hat{z}^{-1} \qquad (M_{10}) \qquad (36)$$

This completes the search for first approximations for ϵ, $\bar{u}_z$, T, and F, but it is now clear from our present results that a continuing process is possible in which mean quantities have the form $\epsilon = \epsilon_+ + R_\tau^{-\frac{1}{2}}\epsilon_{*0} + R_\tau^{-1}\epsilon_{*1} + \ldots$, $F = F_+ + F_{*0} + R_\tau^{-\frac{1}{2}}F_{*1} + \ldots$ etc. where ϵ_{*1}, F_{*1} are functions of $\hat{z}$, and that we may go on to higher approximations.

We have seen so far that T is of the form $T = \chi_0(\zeta) + R_\tau^{-1}\chi_1(\zeta)$ in the outer region (M_0), and the energy equation indicates that $\epsilon = L_0(\zeta)R_\tau^{-1} + L_1(\zeta)R_\tau^{-2}$, that $S = z\bar{u}_z$ and F are of similar forms and, in

general, that all four quantities are expandable in infinite series in R_τ^{-1}. The next approximations are obtained from the matching,

$$S_+ + S_{*0} + R_\tau^{-\frac{1}{2}} S_{*1} + \ldots = \varphi_0 + \varphi_1 R_\tau^{-1} + \ldots \qquad (M_{10}) \qquad (37)$$

$$T_+ + R_\tau^{-\frac{1}{2}} T_{*0} + R_\tau^{-1} T_{*1} + \ldots = 1 - \zeta + \chi_1 R_\tau^{-1} + \chi_2 R_\tau^{-2} + \ldots \qquad (M_{10}) \qquad (38)$$

$$F_+ + F_{*0} + R_\tau^{-\frac{1}{2}} F_{*1} + \ldots = \Lambda_0 + \Lambda_1 R_\tau^{-1} + \ldots \qquad (M_{10}) \qquad (39)$$

$$\epsilon_+ + R_\tau^{-\frac{1}{2}} \epsilon_{*0} + R_\tau^{-1} \epsilon_{*1} + \ldots = L_0 R_\tau^{-1} + L_1 R_\tau^{-2} + \ldots \qquad (M_{10}) \qquad (40)$$

Retaining the first three terms on the left of (37) and two terms on the right and cross-differentiating to eliminate first S_+ and then S_{*0}, we find an equation of the form

$$\tfrac{1}{4} R_\tau^{-\frac{1}{2}} (S_{*1} + S'_{*1} \hat{z}) = H_0(\zeta) + R_\tau^{-1} H_1(\zeta) \qquad (M_{10}) \qquad (41)$$

so that

$$S_{*1} + \hat{z} S'_{*1} = 2C_{10}\hat{z} + K_2 \hat{z}^{-1}, \quad S_{*1} = C_{10}\hat{z} + C_{11}\hat{z}^{-1} + K_2 \hat{z}^{-1} \ell n \hat{z} \qquad (M_{10})$$

where C_{10}, C_{11}, K_2 are constants. Eq. (37) is now of the form

$$S_+ + S_{*0} + K_2 R_\tau^{-\frac{1}{2}} \hat{z}^{-1} \ell n \hat{z} = H_{00}(\zeta) + R_\tau^{-1} H_{10}(\zeta) \qquad (M_{10})$$

Eliminating S_+ and solving for S_{*0}, we get

$$S_{*0} = K_4 \ell n \hat{z} + C_{01}\hat{z}^{-2} + C_{00} \qquad (M_{10})$$

where K_4, C_{01}, C_{00} are constants. Then

$$S_+ = C_0 + C_1 z^{-1}, \quad K_4 = K_2 = 0 \qquad (z \gg 1)$$

where C_0, C_1 are constants. Continuing in this way for all the quantities in (37) and (39), we obtain

$$S_+ = C_0 + C_1 z^{-1} + C_2 z^{-2} + \ldots \qquad (z >> 1) \qquad (42)$$

$$S_{*0} = C_{00} + C_{01}\hat{z}^{-2} + C_{02}\hat{z}^{-4} + \ldots \qquad (M_{10}) \qquad (43)$$

$$S_{*1} = C_{10}\hat{z} + C_{11}\hat{z}^{-1} + C_{12}\hat{z}^{-3} + \ldots \qquad (M_{10}) \qquad (44)$$

...

$$F_+ = D_0 + D_1 z^{-1} + D_2 z^{-2} + \dots \qquad (z \gg 1) \qquad (45)$$

$$F_{*0} = D_{00} + D_{01}\hat{z}^{-2} + D_{02}\hat{z}^{-4} + \dots \qquad (M_{10}) \qquad (46)$$

$$F_{*1} = D_{10}\hat{z} + D_{11}\hat{z}^{-1} + D_{12}\hat{z}^{-3} + \dots \qquad (M_{10}) \qquad (47)$$

$\dots$

If we multiply Eq. (40) by z, we obtain by an identical argument

$$\epsilon_+ = E_0 z^{-1} + E_1 z^{-2} + E_2 z^{-3} + \dots \qquad (z >> 1) \qquad (48)$$

$$\epsilon_{*0} = E_{00}\hat{z}^{-1} + E_{01}\hat{z}^{-3} + \dots \qquad (M_{10}) \qquad (49)$$

$$\epsilon_{*1} = E_{10} + E_{11}\hat{z}^{-2} + \dots \qquad (M_{10}) \qquad (50)$$

$\dots$

Similar arguments applied to (38) yield

$$T_+ = B_0 + B_1 z^{-1} + B_2 z^{-2} + \dots \qquad (z >> 1) \qquad (51)$$

$$T_{*0} = B_{00}\hat{z} + B_{01}\hat{z}^{-1} + B_{02}\hat{z}^{-3} + \dots \qquad (M_{10}) \qquad (52)$$

$$T_{*1} = B_{10} + B_{11}\hat{z}^{-2} + \dots \qquad (M_{10}) \qquad (53)$$

$\dots$

where (5), (32) and the difference between (30) and (32) yield a number of relations among the constants including

$$E_0 = C_0, \quad E_1 = C_1 - C_0^2 - D_1, \quad E_{00} = C_{00}, \quad E_{01} = C_{01} - 2D_{01}$$

$$B_0 = 1, \quad B_1 = -C_0, \quad B_2 = -C_1, \quad B_{00} = -1, \quad B_{01} = -C_{00}, \quad B_{02} = -C_{01}$$

$$B_{10} = -C_{10}, \quad B_{11} = -C_{11}, \quad B_{20} = -C_{20}, \quad B_{21} = -C_{21}, \dots$$

In outer variables we get, to first order,

$$S = C_0 + C_{00} + C_{10}\zeta + C_{20}\zeta^2 + \dots \qquad (M_{10}) \qquad (54)$$

$$F = D_{00} + D_0 + D_{10}\zeta + D_{20}\zeta^2 + \dots \qquad (M_{10}) \qquad (55)$$

$$\epsilon R_\tau = (C_{00} + C_0)\zeta^{-1} + E_{10} + E_{20}\zeta + \dots \qquad (M_{10}) \qquad (56)$$

The mean velocity field is given by

$$u_0 = A_{12} + C_+ + C_* + (C_0 + \tfrac{1}{2}C_{00}) \ell n\, R_\tau + K_{11} R_\tau^{-\frac{1}{2}} + K_{12} R_\tau^{-1} + \dots \qquad (57)$$

$$u_o - \bar{u} = A_{12} - (C_o + C_{oo}) \ln \zeta - C_{10}\zeta - \tfrac{1}{2}C_{20}\zeta^2 + \ldots \qquad (M_{1o}) \qquad (58)$$

$$\bar{u}_+ = C_+ + C_o \ln z - C_1 z^{-1} - \tfrac{1}{2}C_2 z^{-2} - \tfrac{1}{3}C_3 z^{-3} - \ldots \qquad (z \gg 1) \qquad (59)$$

An attempt was made to compute the constants from published data. The solution in (57) for u_o was fitted to the data of Perry and Abell (1977) to obtain $A_{12} + C_+ + C_+ = 4.135$, $(C_o + \frac{1}{2}C_{oo}) = 2.495$, $K_{11} = 2.355$. The comparison is shown in Fig. 1. Next the velocity-defect law in (58) was fitted to the data of Perry and Abell as seen in Fig. 2. This yielded $A_{12} = 1.56$, $C_{10} = 2.03$, $(C_o + C_{oo}) = 2.37$ so that $C_o = 2.62$, $C_{oo} = -0.25$. From the data of Laufer (1954, his Fig. 20), we see that the prediction that $dF/d\zeta$ is constant agrees well with measurements and we estimated $D_{10} = 2$. We now have the constants in the first two terms in (56):

$$\varepsilon R_T = 1.66 + \frac{2.37}{\zeta} \qquad (M_{1o}) \qquad (60)$$

This may be compared to the estimations of Laufer for εR_T. For the higher Reynolds number and at smaller ζ the agreement is excellent, for example 23.0 vs. 25.36 at $\zeta = 0.1$, 13.5 vs. 13.51 at $\zeta = 0.2$ and 9.0 vs. 9.56 at $\zeta = 0.3$. The measurements of εR_T for Laufer's low Reynolds number case are about 15-20% lower than these three predictions. The inner solution for the mean velocity was fitted to the data of Laufer to yield $C_1 = 25.58$, $C_+ = 4.37$. The comparison is shown in Fig. 3. We now estimate D_1 from Laufer (his Fig. 19) by estimating the rather small difference between the pressure and the kinetic-energy diffusion terms. Very roughly we get $D_1 = 6$. We now have the constants in the first two terms of (48):

$$\varepsilon_+ = 2.62z^{-1} + 12.7z^{-2} \qquad (z \gg 1) \qquad (61)$$

This agrees rather well with the data for ε in Laufer's Fig. 19 for $z > 20$. We

conclude our comparison with T_+ in (51). The result

$$T_+ = 1 - 2.62\, z^{-1} - 25.58\, z^{-2} \qquad (z \gg 1) \qquad (62)$$

agrees well with Laufer's Fig. 26 for $z > 10$.

Solutions for root-mean-square velocities and mean pressure.

We have found estimates to first order of rms velocities and turbulence length scales in the mesolayer: $L_x \sim L_y \sim R_\tau$, $L_z \sim R_\tau^{\frac{1}{2}}$, $\sigma_{u2} \sim \sigma_{v2} \sim 1$, $\sigma_{w2} \sim R_\tau^{-\frac{1}{2}}$. We therefore write

$$\sigma_u = f_1(z) + f_{*10} + h_{11} f_{*11} + h_{12} f_{*12} + \ldots \qquad (M_1) \qquad (63)$$

$$\sigma_v = f_2(z) + f_{*20} + h_{21} f_{*21} + h_{22} f_{*22} + \ldots \qquad (M_1) \qquad (64)$$

$$\sigma_w = f_3(z) + R_\tau^{-\frac{1}{2}} f_{*30} + h_{31} f_{*31} + h_{32} f_{*32} + \ldots \qquad (M_1) \qquad (65)$$

where $h_{ij} = h_{ij}(R_\tau)$ and $f_{*ij} = f_{*ij}(\hat{z})$. We also need Eq. (6), which we may write, to first order, as two equations,

$$\begin{aligned} R_\tau^{-\frac{1}{2}}(1-\zeta)\, & h_{40}\bar{p}'_{*0} + h_{41}\bar{p}'_{*1} + \ldots + 2R_\tau^{-\frac{1}{2}} f_3 f'_{*30} + 2f_3' f_{*30} + 2R_\tau^{-1} f_{*30} f'_{*30} \\ & + 2R_\tau^{-\frac{1}{2}} f_3' h_{31} f_{*31} + 2 f_3 h_{31} f'_{*31} + \ldots \\ = R_\tau^{-1} & f_3 f_3' - f_2 f_2' + 2 f_3 f_{*30} R_\tau^{-\frac{1}{2}} + R_\tau^{-1} f_{*30}^2 + 2 f_3 h_{31} f_{*31} + \ldots \qquad (M_1) \qquad (66) \\ & - 2 f_2 f_{*20} - f_{*20}^2 - 2 f_2 f_{*21} h_{21} - \ldots \end{aligned}$$

$$\bar{p}'_+ + 2 f_3 f_3' = 0 \qquad (67)$$

where we have used

$$\bar{p} = \bar{p}_+(z) + h_{40}(R_\tau)\bar{p}_{*0}(\hat{z}) + h_{41}(R_\tau)\bar{p}_{*1}(\hat{z}) + \ldots \qquad (M_1) \qquad (68)$$

Evaluating (66) in the mesolayer, we get $h_{40} = R_\tau^{-\frac{1}{2}}$, $h_{41} = R_\tau^{-1}$, $\ldots$, $h_{31} = R_\tau^{-1}$, $h_{32} = R_\tau^{-\frac{3}{2}}$, $\ldots$, $h_{11} = h_{21} = R_\tau^{-\frac{1}{2}}$, $h_{12} = h_{22} = R_\tau^{-1}$ $\ldots$. In the outer region (M_0), using

$$\sigma_u = F_{10}(\zeta) + \ell_{11}(R_\tau) F_{11}(\zeta) + \ldots \qquad (M_0) \qquad (69)$$

$$\sigma_v = F_{20}(\zeta) + \ell_{21}(R_\tau) F_{21}(\zeta) + \ldots \qquad (M_0) \qquad (70)$$

$$\sigma_w = F_{30}(\zeta) + \ell_{31}(R_\tau) F_{31}(\zeta) + \ldots \qquad (M_0) \qquad (71)$$

$$\bar{p} = F_{40}(\zeta) + \ell_{41}(R_\tau) F_{41}(\zeta) + \ldots \qquad (M_0) \qquad (72)$$

we see that Eq. (6) becomes

$$(1-\zeta) F'_{40} + \ell_{41} F'_{41} + \ldots 2F_{30}F'_{30} + 2F'_{30}F_{31}\ell_{31} + 2\ell_{31}F_{30}F'_{31} + \ldots$$
$$(M_1) \qquad (73)$$
$$= F^2_{30} + 2F_{30}F_{31}\ell_{31} + \ell^2_{31}F^2_{31} + \ldots - F^2_{20} - 2F_{20}\ell_{21}F_{21} - \ell^2_{21}F^2_{21} \ldots$$

so that $\ell_{41} = \ell_{31} = \ell_{21}$, $\ell_{42} = \ell_{32} = \ell_{22} = \ell^2_{31} = \ell^2_{21}$, ...

We have found that the energy flux in the region $z \gg 1$ and $R_\tau = \infty$ is $F_+ = D_0 + D_1 z^{-1} + \ldots$. Since correlation coefficients in this region must be of order one to first order, we get

$$f_3 f_1^2 = \text{const} + \text{const}\ z^{-1} + \ldots \quad (z \gg 1) \qquad (74)$$

$$f_3 = \alpha_{31} + \alpha_{32} z^{-1} + \ldots \qquad (z \gg 1) \qquad (75)$$

$$f_1 = \alpha_{11} + \alpha_{12} z^{-1} + \ldots \qquad (z \gg 1) \qquad (76)$$

These reveal that $\ell_{11} \sim \ell_{21} \sim \ell_{31} \sim R_\tau^{-1}$, ... and the outer forms for σ_u, σ_v, σ_w, $\bar{p}$ are revealed. We match

$$\alpha_{11} + \alpha_{12} z^{-1} + \alpha_{13} z^{-2} + \ldots + f_{*10}(\hat{z}) + R_\tau^{-\frac{1}{2}} f_{*11}(\hat{z}) + \ldots$$
$$(M_{10}) \qquad (77)$$
$$= F_{10}(\zeta) + R_\tau^{-1} F_{11}(\zeta) + \ldots$$

and similar expressions for σ_v, σ_w and $\bar{p}$. The results are

$$\sigma_u = \alpha_{11} + \beta_{11} + \beta_{12}\zeta + \beta_{13}\zeta^2 + \ldots \qquad (M_{10}) \qquad (78)$$

$$\sigma_{u+} = \alpha_{11} + \alpha_{12} z^{-1} + \alpha_{13} z^{-2} + \ldots \qquad (z \gg 1) \qquad (79)$$

$$\sigma_v = \alpha_{21} + \beta_{21} + \beta_{22}\zeta + \beta_{23}\zeta^2 + \ldots \qquad (M_{10}) \qquad (80)$$

$$\sigma_{v+} = \alpha_{21} + \alpha_{22} z^{-1} + \alpha_{23} z^{-2} + \ldots \qquad (z \gg 1) \qquad (81)$$

$$\sigma_w = \alpha_{31} + \beta_{31} + \beta_{32}\zeta + \beta_{33}\zeta^2 + \ldots \qquad (M_{10}) \qquad (82)$$

$$\sigma_{w+} = \alpha_{31} + \alpha_{32} z^{-1} + \alpha_{33} z^{-2} + \ldots \qquad (z \gg 1) \qquad (83)$$

$$\bar{p} = \beta_{41} + \beta_{42}\zeta + \beta_{43}\zeta^2 + \ldots \qquad (M_{10}) \qquad (84)$$

$$\bar{p}_+ = \alpha_{41} + \alpha_{42} z^{-1} + \alpha_{43} z^{-2} + \ldots \qquad (z \gg 1) \qquad (85)$$

The constants in (78)-(83) were estimated using the data of Perry and Abell (1975) for the outer quantities and σ_{w+}, and Laufer (1954) for σ_{v+} and σ_{w+}. The results are

$$\alpha_{11} = 2.1 \ , \ \alpha_{12} = 2.4, \ \alpha_{13} = 330 \qquad (86)$$

$$\beta_{11} = 0.13, \ \beta_{12} = -1.534, \ \beta_{13} = 0.108 \qquad (87)$$

$$\alpha_{21} \cong 1.70, \ \alpha_{22} = -1.08, \ \alpha_{23} = -78 \qquad (88)$$

$$\beta_{21} \cong 0 , \quad \beta_{22} = -1.48, \ \beta_{23} = 0.533 \qquad (89)$$

$$\alpha_{31} = 1.07, \ \alpha_{32} = -10.81, \ \alpha_{33} = 52 \qquad (90)$$

$$\beta_{31} \cong 0 , \quad \beta_{32} = -0.325, \ \beta_{33} = -0.0417 \qquad (91)$$

The comparison with the data are shown in Figs. 4-9.

As indicated by Figs. 4, 5 and 10, σ_u increases very rapidly to a peak at $z \cong 15$ and then decreases gradually in terms of inner variables and sharply in terms of outer variables. The region before the peak may be regarded roughly as the region in which $\bar{u}_z$ is constant so that if we represent σ_u as of order $z\bar{u}_z$, we get the strong linear increase observed. In this region the production term in the energy equation which produces u-fluctuations only increases σ_u and has a minor effect on σ_v and σ_w. This is supported by the data (Laufer, Fig. 25) which show that σ_u^2 is the major part of the total turbulence energy in this region. Just before the peak of σ_u, however, the pressure-scrambling terms in the moment equations (Hinze, 1975, p. 326) begin to create v-and w-fluctuations, σ_u decreases and σ_v, σ_w increase. This behavior is also revealed by the data for $z > 15$. The details of the rms velocity profiles in and near the mesolayer are of great importance but we need first a derivation of the behavior of mean quantities in the region $z \ll R_\tau^{\frac{1}{2}}$.

Behavior of Mean Quantities in the Region $z \ll R_\tau^{\frac{1}{2}}$.

For computational purposes we have assumed above that there is a region (at least for large R_τ) in which $\bar{u}_+$, σ_{u+}, ... are good approximations to $\bar{u}$, σ_u, ..., and this is a good assumption because in experiments there are regions in which there is good independence of the outer length (Reynolds number similarity). However, as we increase z and approach the mesolayer, contributions from the mesolayer arise which we may obtain by assuming a Taylor series expansion of the functions of $\hat{z}$, for example, $f_{*10}(\hat{z}) = \alpha_{111}\hat{z} + \alpha_{112}\hat{z}^2 + \ldots$ for $\hat{z} \ll 1$. We get

$$\sigma_u = f_1(z) + \alpha_{111}\hat{z} + \alpha_{112}\hat{z}^2 + \ldots + R_\tau^{-\frac{1}{2}}(\alpha_{121}\hat{z} + \alpha_{122}\hat{z}^2 + \ldots) + \ldots \qquad (0 \le z \ll R_\tau^{\frac{1}{2}}) \tag{92}$$

$$\sigma_v = f_2(z) + \alpha_{211}\hat{z} + \alpha_{212}\hat{z}^2 + \ldots + R_\tau^{-\frac{1}{2}}(\alpha_{221}\hat{z} + \alpha_{222}\hat{z}^2 + \ldots) + \ldots \qquad (0 \le z \ll R_\tau^{\frac{1}{2}}) \tag{93}$$

$$\sigma_w = f_3(z) + R_\tau^{-\frac{1}{2}}(\alpha_{322}\hat{z}^2 + \alpha_{323}\hat{z}^3 + \ldots) + R_\tau^{-1}(\alpha_{332}\hat{z}^2 + \alpha_{333}\hat{z}^3 + \ldots) + \ldots \qquad (0 \le z \ll R_\tau^{\frac{1}{2}}) \tag{94}$$

where we use $\partial\sigma_w/\partial z = 0$ at $z = 0$. Also

$$\epsilon = \epsilon_+(z) + R_\tau^{-\frac{1}{2}}(E_{120} + E_{121}\hat{z} + \ldots) + R_\tau^{-1}(E_{130} + E_{131}\hat{z} + \ldots) + \ldots \qquad (0 \le z \ll R_\tau^{\frac{1}{2}}) \tag{95}$$

$$F = F_+(z) + D_{111}\hat{z} + D_{112}\hat{z}^2 + \ldots + R_\tau^{-\frac{1}{2}}(D_{121}z + D_{122}\hat{z}^2 + \ldots) + \ldots \qquad (0 \le z \ll R_\tau^{\frac{1}{2}}) \tag{96}$$

$$S = S_+(z) - \hat{z}^2 + C_{114}\hat{z}^4 + \ldots + R_\tau^{-\frac{1}{2}}(C_{124}\hat{z}^4 + C_{125}\hat{z}^5 + \ldots) + \ldots \qquad (0 \le z \ll R_\tau^{\frac{1}{2}}) \tag{97}$$

$$T = 1 - z^{-1} S_+(z) - R_\tau^{-\frac{1}{2}} (C_{11_4} \hat{z}^3 + C_{11_5} \hat{z}^4 + \ldots) - R_\tau^{-1} (C_{12_3} \hat{z}^3 + C_{12_4} \hat{z}^4 + \ldots) + \ldots \tag{98}$$

$$(0 \leq z \ll R_\tau^{\frac{1}{2}})$$

where we have used (5) and required that $T = T_z = T_{zz} = 0$ at $z = 0$. Also

$$\bar{u} = \bar{u}_+(z) - \tfrac{1}{2}\hat{z}^2 + \tfrac{1}{3} C_{11_4} \hat{z}^4 + \ldots + R_\tau^{-\frac{1}{2}} (\tfrac{1}{4} C_{12_4} \hat{z}^4 + \tfrac{1}{5} C_{12_5} \hat{z}^5 + \ldots) + \ldots \tag{99}$$

$$(0 \leq z \ll R_\tau^{\frac{1}{2}})$$

The Behavior of Mean Quantities in the Mesolayer.

We may now infer the behavior of mean quantities in the mesolayer itself. According to theory and measurements in shear-free turbulence (Hunt and Graham, 1978), we expect the mesolayer to tend to cause an increase(local maxima) in tangential velocities σ_u and σ_v since the wall, in effect, transfers energy from the normal component σ_w to the parallel components. For σ_u the inner behavior involves an additional peak at fixed z near the wall as we have already seen. From (92) we obtain

$$\sigma_u = \sigma_{11} + \sigma_{12} z^{-1} + \ldots + \sigma_{111} \hat{z} + \sigma_{112} \hat{z}^2 + \ldots + R_\tau^{-\frac{1}{2}} \sigma_{121} \hat{z} + \ldots \quad (M_{11}) \tag{100}$$

in a region beyond the inner maximum. Obviously, at very large R_τ, there will be a subregion in M_{11} in which σ_u is nearly constant for a long distance between points T_1 and T_2 in Fig. 10. To the left of T_2 the universal law of the wall is obeyed. On the other hand, at very large z, but not near the center of the pipe, the behavior is Reynolds-number independent and is given by

$$\sigma_u = \sigma_{11} + \delta_{11} + \delta_{12} \zeta \qquad (M_0) \tag{101}$$

as also shown in Fig. 10 to the right of T_4. But nearer the mesolayer,the behavior is

$$\sigma_u = \alpha_{11} + \beta_{11} + \beta_{11,2}\hat{z}^{-2} + \beta_{11,4}\hat{z}^{-4} + \ldots + \beta_{12}\hat{z}\,R_\tau^{-\frac{1}{2}} + \ldots \qquad (M_{10}) \qquad (102)$$

Since we have assumed, on physical grounds, a peak of σ_u in the mesolayer as we move to smaller z along the linear curve of (101), the $\hat{z}^{-2}$-term in (102) begins to be of importance and $\beta_{11,2} < 0$. The slope becomes less and less negative and finally becomes zero (and σ_u becomes a maximum at T_4), as we portray in Fig. 10. Still closer to the wall, there is a region where none of the forms for σ_u in (100)-(102) apply. As we increase z in the region just to the left of T_2 the $\hat{z}$, $\hat{z}^2$, ... terms in (100) begin to be important and the curve turns up as shown to meet the portion to the left of T_4.

We may find the various transition points in Fig. 10. Obviously, in the region between T_2 and T_4 and not close to either, the only important term from the inner solution is the constant term α_{11} and, from the outer region, $f_{*10}(\hat{z})$. Thus

$$\sigma_u = \alpha_{11} + f_{*10}(\hat{z})$$

and the data should collapse when plotted against $\hat{z}$. We see, in fact, a clear tendency for this behavior in the data of Perry and Abell (1975) in Fig. 11 which is plotted against $\hat{z}$. The inflection point T_3 is at fixed $\hat{z}$ which we see from Fig. 11 is approximately 3.0. At T_2 the weak z^{-1}-behavior of the inner solution is matched by the weak $\hat{z}$-behavior of the mesolayer contribution in Eq. (100), i.e. $z^{-1} \sim \hat{z}$ or $z \sim R_\tau^{\frac{1}{4}}$ at the location of T_2. At T_4 the $\hat{z}^{-2}$-term matches the $R_\tau^{-\frac{1}{2}}$-term in (102) and this occurs at $\hat{z} \sim R_\tau^{\frac{1}{8}}$ or $z \sim R_\tau^{\frac{3}{8}}$. The locations of T_2, T_3 and T_4 show why the collapse of the data in Fig. 11 is confined to such a small region at the typical Reynolds number of the experiments.

Not all of the details of this description of σ_u in and near the mesolayer can be verified by experiment because of errors of measurement and too-

low Reynolds numbers but the data of Perry and Abell in Fig. 11 is in remarkable agreement with the general behavior outlined. The data for σ_v from both Laufer and Perry and Abell is less reliable but the theory indicates that a similar behavior occurs but with the peak in the sublayer missing and with α_{22} in (81) negative as we decided in (88). For σ_u, β_{11} is tentatively evaluated as $\beta_{11} \cong 0.13$ in Eq. (87). For σ_v, the data does not permit accurate evaluation of β_{21} and we have set $\beta_{21} = 0$ in Eq. (89).

The outer maximum of σ_u is at $z \sim R_\tau^{\frac{3}{4}}$ but for the typical Reynolds number of experiments this is probably indistinguishable from the mesolayer region $z \sim R_\tau^{\frac{1}{2}}$. This may also be true of σ_v. Very roughly, Laufer's data indicate a peak of σ_v at $z \cong a_2 R_\tau^{\frac{1}{2}}$ where $a_2 \cong 3.0$. The normal component σ_w has a maximum at $z = a_3 R_\tau^{\frac{1}{2}}$ and the data of Laufer and Perry and Abell suggest $a_3 \cong 7.0$. This is as it should be because σ_w is little influenced by the second component of motion in the inner portions of the mesolayer. Because of this, we would also predict that σ_w should show independence of R_τ over a greater distance of the wall region that σ_u and σ_v and this is also revealed by Laufer's data.

The analysis of $\bar{u}$ in the transition is delicate because, as observations show, $\bar{u}$ is so close to logarithmic in a large region. We may arrive at some interesting predictions, however, as follows: We write down the forms for S (which is the slope of $\bar{u}$ in a logarithmic plot) in M_{10} and M_{11} as

$$S = C_0 + C_{00} + C_{01}\hat{z}^{-2} + \ldots \qquad (M_{10}) \qquad (103)$$

$$S = C_0 - \hat{z}^2 + \ldots \qquad (M_{11}) \qquad (104)$$

We also need the outer form of T:

$$T = 1 - \hat{z}\, R_\tau^{-\frac{1}{2}} + (C_0 + C_{\infty 0})\, \hat{z}^{-1} R_\tau^{-\frac{1}{2}} - C_{01}\, \hat{z}^{-3} R_\tau^{-\frac{1}{2}} + \ldots \qquad (M_{10}) \qquad (105)$$

In (105) the $\hat{z}^{-3} R_\tau^{-\frac{1}{2}}$ - term probably contributes negative curvature so that $C_{01} > 0$. A schematic plot of S near the transition region is shown in Fig. 12. The upper dashed line is the classical solution $S = C_0$. For larger $\hat{z}$ and very large R_τ, S is close to $C_0 + C_{00}$ but at smaller $\hat{z}$ the C_{01}-term causes S to increase as shown. The joining requires that C_{00} is negative, perhaps, $C_{00} = -0.25$ as calculated roughly from the data. This behavior suggests a picture of $\bar{u}$ vs. $\ell n\, z$ or $\ell n\, \hat{z}$ in and on both sides of the mesolayer as in the dashed curve of Fig. 13. The data of Perry and Abell (1975) is suggestive of this but the data points are so crowded that one can't be sure. Laufer's data (Rotta, 1962) also has the same trends but again the deviation from logarithmic behavior is weak. The present theory does not apply directly to turbulent boundary layers at zero pressure gradient but a similar theory in preparation (Long and Chen, 1980) has a similar behavior for $\bar{u}$ in and on both sides of the mesolayer. Ueda and Hinze (1975) measured $\bar{u}$ at two Reynolds numbers and both are suggestive of the trends in Fig. 13. Similar measurements of Smith and Walker (1959) appear conclusive. Details are contained in Long and Chen (1980).

4. Comparisons of the Classical and Mesolayer Theories.

A number of authors (Tennekes, 1968, Bush and Fendell, 1972, Afzad and Yajnik, 1973, Afzal, 1976) have gone on to higher approximations using the classical results for the first approximation. If one assumes[1](Afzal, 1976)

$$S = f_0^*(z) + h_1(R_\tau) f_1^*(z) + h_2(R_\tau) f_2^*(z) + \ldots \tag{106}$$

$$T = g_0^*(z) + \ell_1(R_\tau) g_1^*(z) + \ell_2(R_\tau) g_2^*(z) + \ldots \tag{107}$$

for the inner expansion and

$$S = \varphi_0(\zeta) + m_1(R_\tau)\varphi_1(\zeta) + m_2(R_\tau)\varphi_2(\zeta) + \ldots \tag{108}$$

$$T = \psi_0(\zeta) + n_1(R_\tau)\psi_1(\zeta) + n_2(R_\tau)\psi_2(\zeta) + \ldots \tag{109}$$

for the outer expansion, then, substituting into (5) we see that $h_1 = \ell_1 = m_1 = n_1 = R_\tau^{-1}$ or

$$S = f_0^* + R_\tau^{-1} f_1^* + R_\tau^{-2} f_2^* + \ldots \tag{110}$$

$$T = g_0^* + R_\tau^{-1} g_1^* + R_\tau^{-2} g_2^* + \ldots \tag{111}$$

and

$$S = \varphi_0 + R_\tau^{-1}\varphi_1 + R_\tau^{-2}\varphi_2 + \ldots \tag{112}$$

$$T = \psi_0 + R_\tau^{-1}\psi_1 + R_\tau^{-2}\psi_2 + \ldots \tag{113}$$

Matching yields

$$S = C_0 + A_{01} z^{-1} + A_{02} z^{-2} + \ldots + R_\tau^{-1}(A_{10} z + A_{11} + A_{12} z^{-1} + \ldots) + R_\tau^{-2}(A_{20} z^2 + A_{21} z + A_{22} + \ldots) + \ldots \tag{114}$$

[1]The forms in (106)-(109) follow from the universal law of the wall and Reynolds number similarity and the assumptions that in regions $z \sim 1$ and $\zeta \sim 1$ mean quantities have the same order of magnitude at each point. Afzal's work seems to be the most recent of these efforts and he claims to include earlier work as special cases. One may search for other routes to higher approximations in hopes of rescuing the classical first approximation. I don't know how to make an exhaustive search, however, and I will be content in this paper to advance the new theory as best I can and, in the arguments of this section, to transfer the burden of proof to anyone still favoring the earlier theory.

We may, in fact, use the concept of the mesolayer as a layer of transition from inner to outer behavior for the Reynolds stress T to derive the thickness of the mesolayer without reference to the "eddy-sloshing" argument of Section 2. We accept as sufficiently general the following forms of the shear-function S and Reynolds stress T, in which the similarity variable $\hat{z}$ is now $\hat{z} = z/R_\tau^b$ and M_1, M_0 are now $0 \leq z \ll R_\tau$ and $R_\tau^b \ll z \leq R_\tau$:

$$S = S_+(z) + \sum_{i=1}^{\infty} R_\tau^{-s_i} S_{*i}(\hat{z}) \qquad (M_1) \qquad (116)$$

$$S = \varphi_0(\zeta) + \sum_{i=1}^{\infty} R_\tau^{-a_i} \varphi_i(\zeta) \qquad (M_0) \qquad (117)$$

$$T = T_+(z) + \sum_{i=1}^{\infty} R_\tau^{-t_i} T_{*i}(\hat{z}) \qquad (M_1) \qquad (118)$$

$$T = \chi_0(\zeta) + \sum_{i=1}^{\infty} R_\tau^{-b_i} \chi_i(\zeta) \qquad (M_0) \qquad (119)$$

where $s_{i+1} > s_i$, $a_{i+1} > a_i$, ... Using $a = (1-b)^{-1}$, matching yields

$$S_+ = A_0 + \sum_{i=1}^{\infty} A_i z^{-a_i}, \quad T_+ = B_0 + \sum_{i=1}^{\infty} B_i z^{-b_i} \qquad (120)$$

$$\varphi_0 = A_0 + \sum_{i=1}^{\infty} A_{*i0} \zeta^{as_i}, \quad \chi_0 = B_0 + \sum_{i=1}^{\infty} B_{*i0} \zeta^{at_i} \qquad (121)$$

$$S_{*i} = A_{*i0} \hat{z}^{as_i} + \sum_{j=1}^{\infty} A_{*ij} \hat{z}^{a(s_i - a_j)} \qquad (122)$$

$$\varphi_i = \sum_{j=1}^{\infty} A_{*ji} \zeta^{a(s_j - a_i)} + A_i \zeta^{-a_i} \qquad (123)$$

$$T_{*i} = B_{*i0} \hat{z}^{at_i} + \sum_{j=1}^{\infty} B_{*ij} \hat{z}^{a(t_i - b_j)} \qquad (124)$$

$$\chi_i = \sum_{j=1}^{\infty} B_{*ji} \zeta^{a(t_j - b_i)} + B_i \zeta^{-b_i} \qquad (125)$$

Substitution into Eq. (5) yields

$$b_1 = 1,\ b_{i+1} = 1+a_i,\ t_1 = 1-b,\ s_1 = 1-2b,\ t_i = s_i + b \tag{126}$$

We obtain, for example, for larger $\hat{z}$

$$T = 1 - C_0 z^{-1} + B_2 z^{-b_2} + \ldots + R_\tau^{-1+b}(-\hat{z} + B_{*11}\hat{z}^{-ab} + \ldots) \tag{127}$$

$$+ R_\tau^{-b-s_2}(B_{*21}\hat{z}^{a(s_2+b-1)} + \ldots) + \ldots$$

and for smaller $\hat{z}$,

$$T = 1 - C_0 z^{-1} + B_2 z^{-2} + \ldots + R_\tau^{-1+b}(A_{30}\hat{z}^3 + \ldots) + \ldots \tag{128}$$

We find in either case that the existence of a transition region $\hat{z} \sim 1$ requires $b = \frac{1}{2}$ or $z \sim R_\tau^{\frac{1}{2}}$ as in the "eddy-sloshing" argument of Section 2.

We may now conveniently discuss the third basic assumption of classical theory (Tennekes and Lumley, 1972, p. 146 and p. 265) that there is a finite region of overlap of the inner and outer regions. According to Tennekes and Lumley and, indeed, the basic concept of an overlap region, ν should first become important at large R_τ at some $z \sim 1$ as we move toward the wall, and H should first become important at some $z \sim H$ as we move outward. As portrayed in Fig. 14, the overlap region at high R_τ is the double-hatched region. In the present theory a transition region replaces the region of overlap. Here both ν and H are important but H decreases in importance as z decreases within the region and ν decreases in importance as z increases in the region. The situation is then as pictured in Fig. 15.

Malkus (1979) has stated that an overlap "is not required by either logic or

dynamics". Nevertheless, our finding that viscosity has importance in a layer much great in thickness than the sublayer needs explanation. We may extend an argument first advanced to me by my student, C.S. Chern, who, together with the present author, extended the mesolayer concept to the problem of thermal convection over a hot surface (Chern and Long, 1980). In this case, we find a mesolayer thickness $\delta_m \sim K^{\frac{1}{2}} H^{\frac{1}{3}} q^{-\frac{1}{6}}$, where K is the coefficient of molecular diffusion, H is the depth of the fluid and q is the buoyancy flux. Chern argued that a thermal rising from the hot surface would move vertically but also be carried horizontally by the large eddies of size H. Since these have a speed of order $(qH)^{\frac{1}{3}}$, their time scale is $T_e = H^{\frac{2}{3}} q^{-\frac{1}{3}}$ and, if we assume that the thermals expand by thermal conduction, they attain a size $(KT_e)^{\frac{1}{2}}$, which precisely equals the mesolayer thickness δ_m. After that they presumably lose their identity. Thus the transport of heat by these thermals which must be of primary importance in the layer where they exist, i.e. the mesolayer, is influenced directly by molecular conduction because they increase in size by molecular conduction, <u>even when they are far above the sublayer</u>. In shear turbulence, observations indicate the existence of a burst phenomenon, as we have already discussed, and the bursts may play a role similar to that of the thermals. Then, if they also diffuse by molecular processes, their size after a time of the order of the outer eddy time, H/u_τ, is $(\nu H/u_\tau)^{\frac{1}{2}}$, which is again precisely the mesolayer thickness. Such may be the basic importance of viscosity in the mesolayer.

5. Conjectures on Intermittency.

We have conjectured that the viscous mesolayer is the region of origin of the bursts observed in pipe and boundary layer flows. This suggests the existence of three time-scales in this layer. One is the time-scale of the energy-containing eddies. Another is the period of the bursts. This may be identified, perhaps, with the set of equations N_2. We may estimate

$$\frac{\partial u_2}{\partial t} \sim \frac{u_2}{T_b} \sim u_1 \frac{\partial u_2}{\partial x} \sim \frac{u_2}{R_\tau} \tag{129}$$

yielding $T_b \sim R_\tau$ as conjectured by a number of experimenters based on observations (Rao, et al., 1971, Ueda and Hinze, 1975, Heidrick, et al., 1977, Chen and Blackwelder, 1978). A third time scale is the duration of the bursts, T_d. The intermittency of the turbulence may be defined as $\gamma = T_d / T_b$. All observations indicate that the Reynolds stress is provided in major part by the bursts which presumably act as mixing elements so that we may write, in the language of mixing-length theory,

$$\overline{uw} \sim 1 \sim (\gamma L_* u_*) \bar{u}_z \tag{130}$$

where $\gamma L_* u_*$ is the eddy viscosity and we have written L_* for the mixing length and u_* for the velocity of the burst. Estimating $u_* \sim 1$ and writing $\bar{u}_z \sim 1/R_\tau^{\frac{1}{2}}$ we find

$$\gamma \sim R_T^{\frac{1}{2}} / L_e \tag{13'}$$

If we now assume, quite naturally, that the duration of the burst is the time for travel over the mixing length, we get $T_d \sim L_e$. But

$$\gamma \sim \frac{T_d}{T_b} \sim \frac{L_e}{R_T} \sim \frac{R_T^{\frac{1}{2}}}{L_e} \tag{13}$$

so that

$$L_e \sim R_T^{\frac{3}{4}}, \quad \gamma \sim R_T^{-\frac{1}{4}}, \quad T_d \sim R_T^{\frac{3}{4}} \tag{13}$$

The expression for γ yields $\gamma \tilde{=} 0.1 - 0.2$ for typical Reynolds numbers and this is in rough agreement with observations.

Acknowledgements

This research was supported by the Office of Naval Research, Fluid Dynamics Division, under Contract No. N00014-75-C-0805, and by the National Science Foundation, under Grants No. OCE 76-18887 and ATM 76-22284. Some of this work was done while on sabbatical leave at the University of Oslo and at the VHL Laboratory in Trondheim, Norway, and I am indebted especially to Professor Enok Palm in Oslo and to Torkild Carstens and Thomas McClimans in Trondheim. I am also grateful to Mr. C. S. Chern and T. C. Chen for help in analysing the data and for many discussions.

LEGENDS

Figure 1. Theoretical curve for u_o, together with data of Perry and Abell (1977).

Figure 2. Velocity defect law $u_o - \bar{u}$ compared with the data of Perry and Abell (1975).

Figure 3. Mean velocity near the wall. Comparison is with the data of Perry and Abell.

Figure 4. Inner solution for σ_{u+} compared with data of Perry and Abell for highest Reynolds number.

Figure 5. Outer solution for σ_u compared with data of Perry and Abell.

Figure 6. Inner solution for σ_{v+} compared with data of Laufer for the higher Reynolds number.

Figure 7. Outer solution for σ_v compared with data of Laufer.

Figure 8. Inner solution for σ_{w+} compared with data of Laufer.

Figure 9. Outer solution for σ_w compared with data of Perry and Abell.

Figure 10. Schematic picture of σ_u.

Figure 11. Perry and Abell data for σ_u: ∇, $R_\tau^{\frac{1}{2}} = 69$; x, $R_\tau^{\frac{1}{2}} = 58$; $\square$, $R_\tau^{\frac{1}{2}} = 51$; $\circ$, $R_\tau^{\frac{1}{2}} = 40$.

Figure 12. Schematic picture of S near the transition.

Figure 13. Micro-variations of $\mathfrak{u}$ in mesolayer.

Figure 14. Overlap region in classical theory.

Figure 15. Intruding mesolayer.

Afzal, N., 1976 Millikan's argument at moderately large Reynolds number. Physics Fluids, 19, 600-602.

Afzal, N. and Yajnik, K., 1973 Analysis of turbulent pipe and channel flows at moderately large Reynolds numbers. J. Fluid Mech., 61, 23-31.

Bullock, K. J., Cooper, R. E., and Abernathy, F. H., 1978 Structural similarity in radial correlations and spectra of longitudinal velocity fluctuations in pipe flow. J. Fluid Mech., 88, 585-608.

Bush, W. B., and Fendell, F. E., 1972 Asymptotic analysis of turbulent channel and boundary-layer flow. J. Fluid Mech., 56, 657-681.

Businger, J. A., Wyngaard, J. C., Izumi, Y., and Bradley, E. F., 1971 Flux profile relationships in the atmospheric surface layer. J. Atmos. Sci. 28, 181-189.

Chen, C.-H., and Blackwelder, R. F., 1978 Large-scale motion in a turbulent boundary layer: a study using temperature contamination. J. Fluid Mech., 89, 1-32.

Chern, C.S., and Long, R. R., 1980 A new theory of turbulent convection. (In preparation)

Fritsch, W., 1928 Einfluss der Wandrauhigkeit auf die turbulente Geschwindigkeit-Verteilung in Rinnen, Zs. angew. Math., Mech., 8, No. 2, 199-216.

Heidrick, T. R., Banerjee, S., and Azad, R. S., 1977 Experiments on the structure of turbulence in fully developed pipe flow. Part 2. A statistical procedure for identifying "bursts" in the wall layers and some characteristics of flow during bursting periods. J. Fluid Mech., 82, 705-723.

Hinze, J. O., 1975 Turbulence, McGraw-Hill, New York.

Hopfinger, E. J., and Toly, M.-A., 1976 Spacially decaying turbulence and its relation to mixing across density interfaces. J. Fluid Mech., 78, 155-175.

Hunt, J. C. R., and Graham, J. M. R., 1978 Free-stream turbulence near plane boundaries. J. Fluid Mech., 84, 209-235.

Izakson, A., 1937 Formula for the velocity distribution near a wall. Zh. Eksper. Teor. Fix., 7, No. 7, 919-924.

Kármán, T. von, 1930 Mechanische Ähnlichkeit und Turbulenz, Nachr. Ges. Wiss Göttingen, Math-Phys. Kl., 58-76.

Laufer, J., 1954 The structure of turbulence in fully developed pipe flow. Nat. Advis. Comm. Aeronautics, Rep. No. 1174.

Laufer, J. and Badri Narayanan, M. A., 1971 Mean period of the turbulent production mechanism in a boundary layer. Phys. Fluids, 14, 182-183.

Long, R. R., and Chen, T. C., 1980 A new theory of the turbulent boundary layer in zero pressure gradient. (In preparation).

Long, R. R., 1978 A theory of mixing in a stably stratified fluid. J. Fluid Mech., 84, 113-124.

Malkus, W. V. R., 1979 Turbulent velocity profiles from stability criteria. J. Fluid Mech., 90, 401-414.

Millikan, C. B., 1938 A critical discussion of turbulent flows in channels and circular tubes. Proc. 5th Intern. Congr. Appl. Mech., Cambridge (USA), 386-392.

Mitchell, J. E., and Hanratty, T. J., 1966 A study of turbulence at a wall using an electrochemical wall shear-stress meter. J. Fluid Mech., 26, 199-221.

Monin, A. S. and Yaglom, A. M., 1971 Statistical Fluid Mechanics. I. Mechanics of Turbulence, MIT Press.

Perry, A. E., and Abell, C. J., 1975 Scaling laws for pipe flow turbulence. J. Fluid Mech., 67, 257-271.

_____, 1977 Asymptotic similarity of turbulence structure in smooth-and rough-walled pipes. J. Fluid Mech., 79, 785-791.

Prandtl, L., 1925 Bericht über Untersuchungen zur ausgebildeten Turbulenz, Zs. angew Math., Mech., 5, No. 2, 136-139.

_____, 1932 Zur turbulenten Strömung in Röhren and längs Platten, Ergebn. Aerodyn. Vesuchsanst, Göttingen, 4, 18-29.

Rao, K. Narahari, Narasimha, R., and Badri Narayanan, M. A., 1971 The "bursting" phenomenon in a turbulent boundary layer. J. Fluid Mech., 48, 339-352.

Rotta, J. C., 1962 Turbulent boundary layers in incompressible flow. Progress in Aeronautical Sciences 2, 1-220.

Smith, D. W., and Walker, J. H., 1959 Skin-friction measurements in incompressible flow. NASA Rep. R-26.

Tennekes, H., 1968 Outline of a second-order theory of turbulent pipe flow. J. AIAA, 6, 1735-1740.

Tennekes, H., and Lumley, J. L., 1972 A First Course in Turbulence, MIT Press.

Thomas, N. H., and Hancock, D. E., 1977 Grid turbulence near a moving wall. J. Fluid Mech., 82, 481-496.

Townsend, A. A., 1976 The Structure of Turbulent Shear Flow, Cambridge Univ. Press.

Tritton, D. J., 1967 Some new correlation measurements in a turbulent boundary layer. J. Fluid Mech., 28, 439-62.

Ueda, H., and Hinze, J. O., 1975 Fine-structure turbulence in the wall region of a turbulent boundary layer. J. Fluid Mech., 67, 125-143.

Uzkan, T. and Reynolds, W. C., 1967 A shear-free turbulent boundary layer. J. Fluid Mech. 28, 803-821.

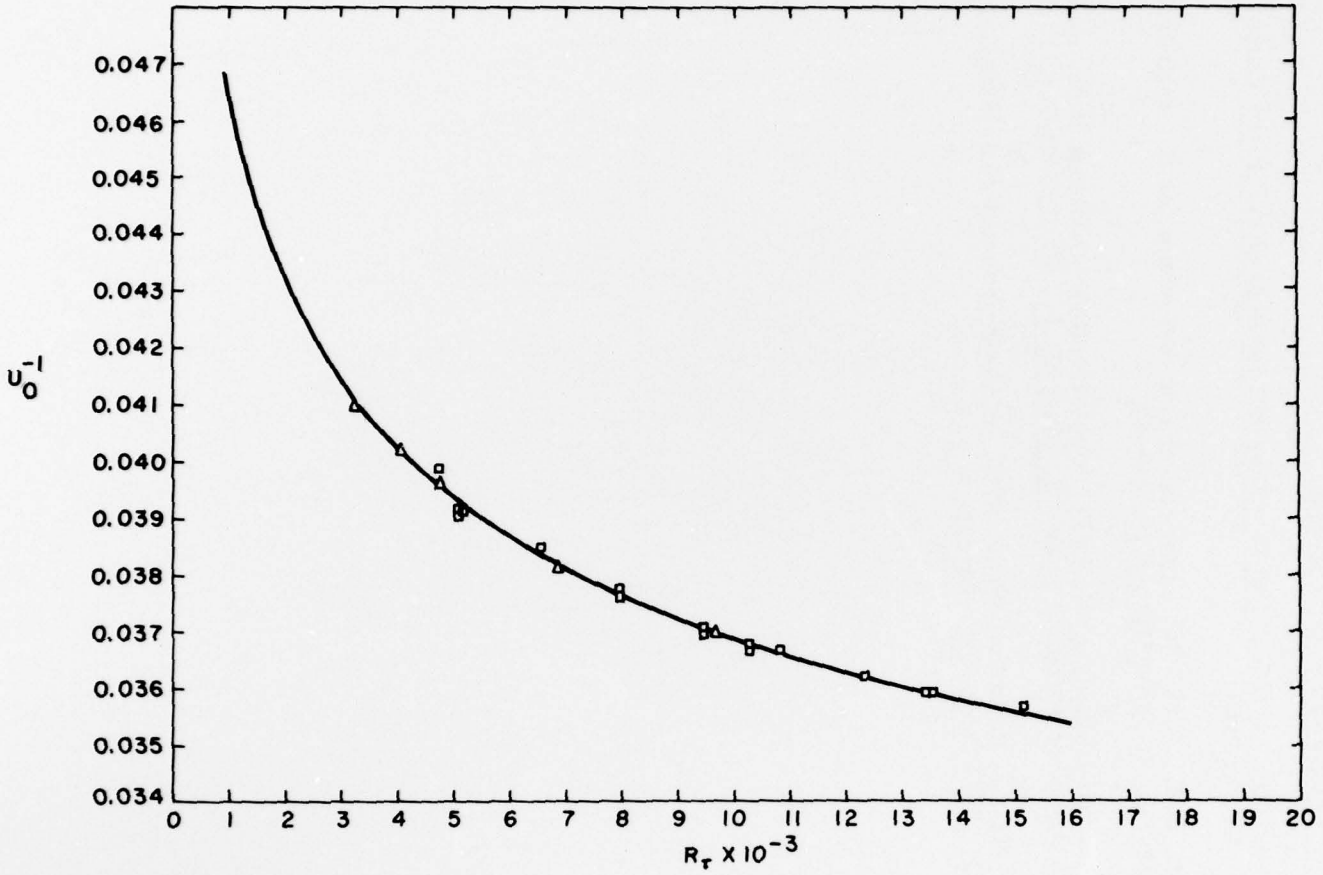
0.047
0.046
0.045
0.044
0.043
0.042
0.041
0.040
0.039
0.038
0.037
0.036
0.035
0.034
U_0^{-1}
0 1 2 3 4 5 6 7 8 9 10 11 12 13 14 15 16 17 18 19 20
$R_\tau \times 10^{-3}$

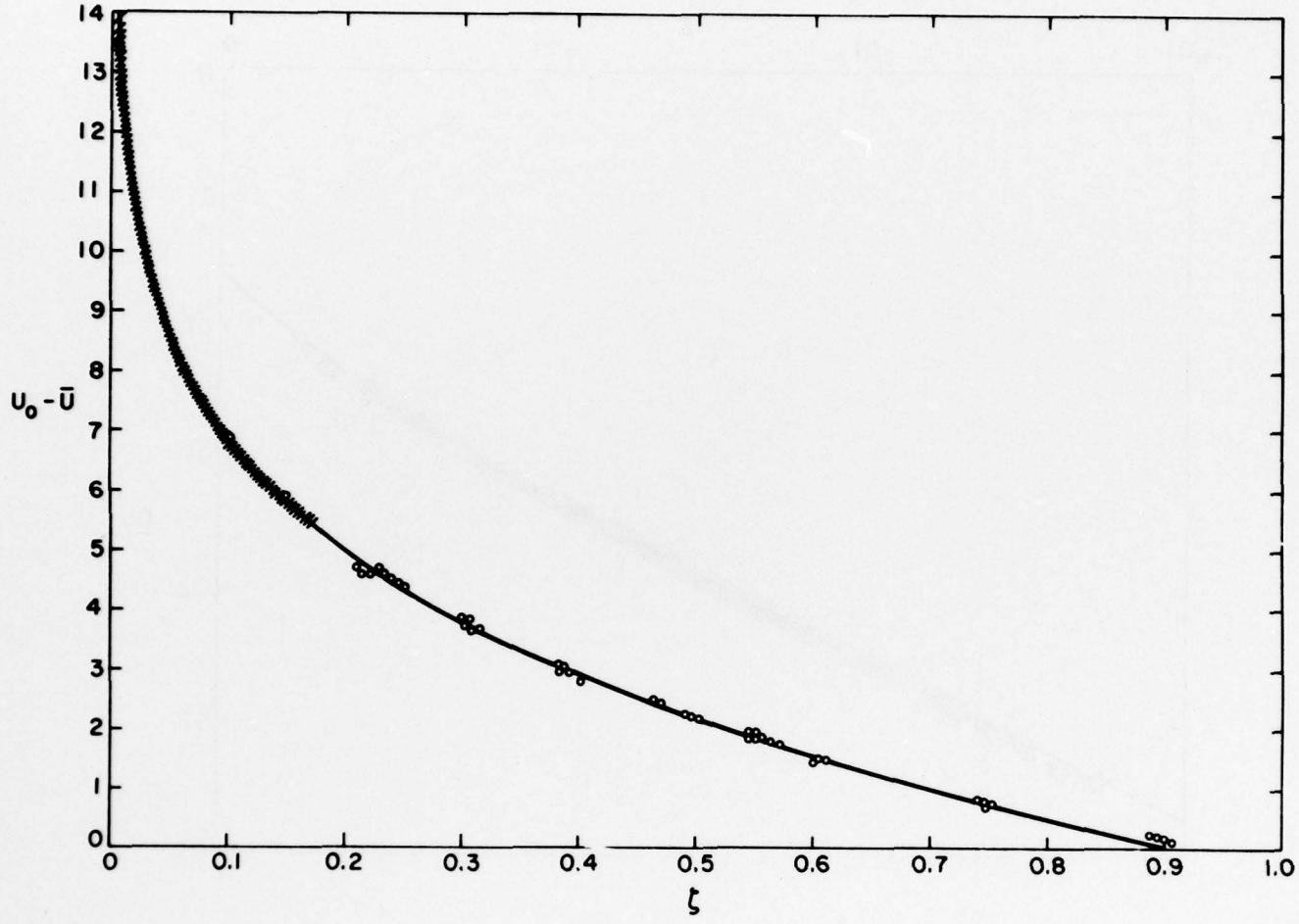
14
13
12
11
10
9
8
7
6
5
4
3
2
1
0
$U_0 - \bar{U}$
0
0.1
0.2
0.3
0.4
0.5
0.6
0.7
0.8
0.9
1.0
ζ

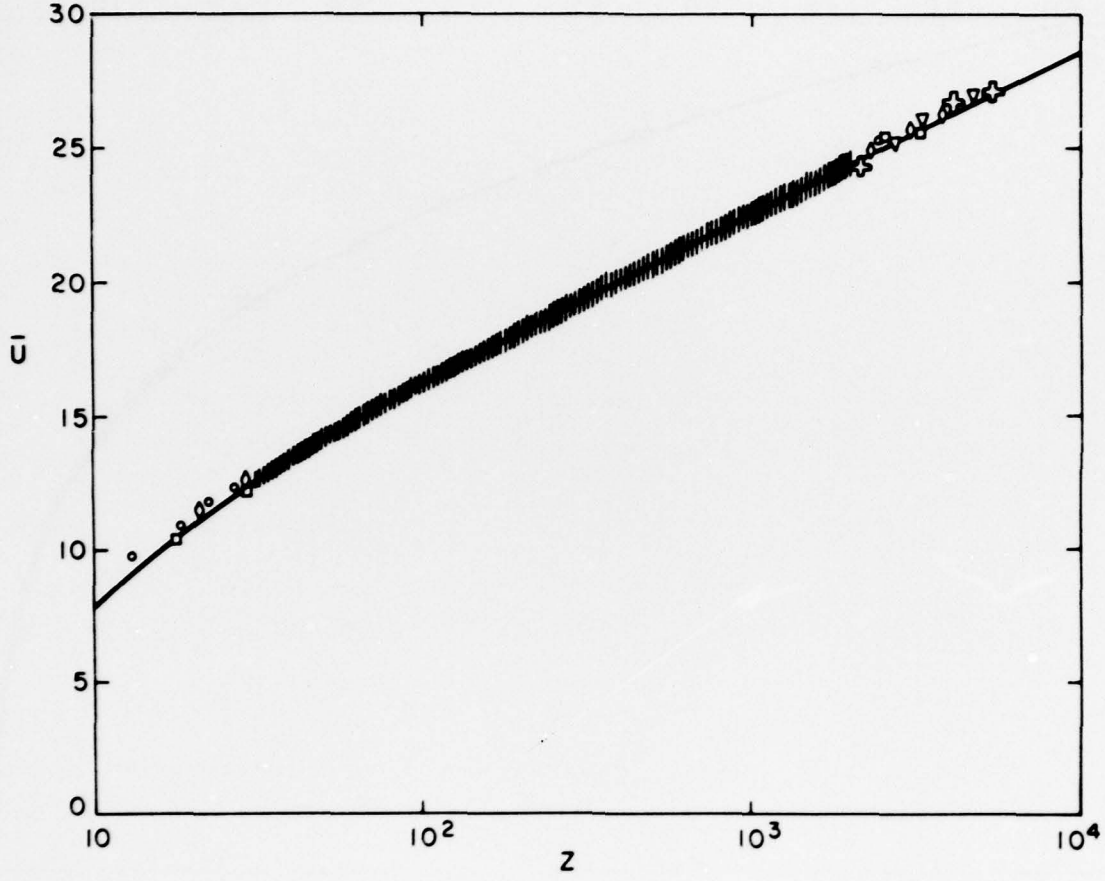
30
25
20
15
10
5
0
$\bar{U}$
10
10^2
10^3
10^4
Z

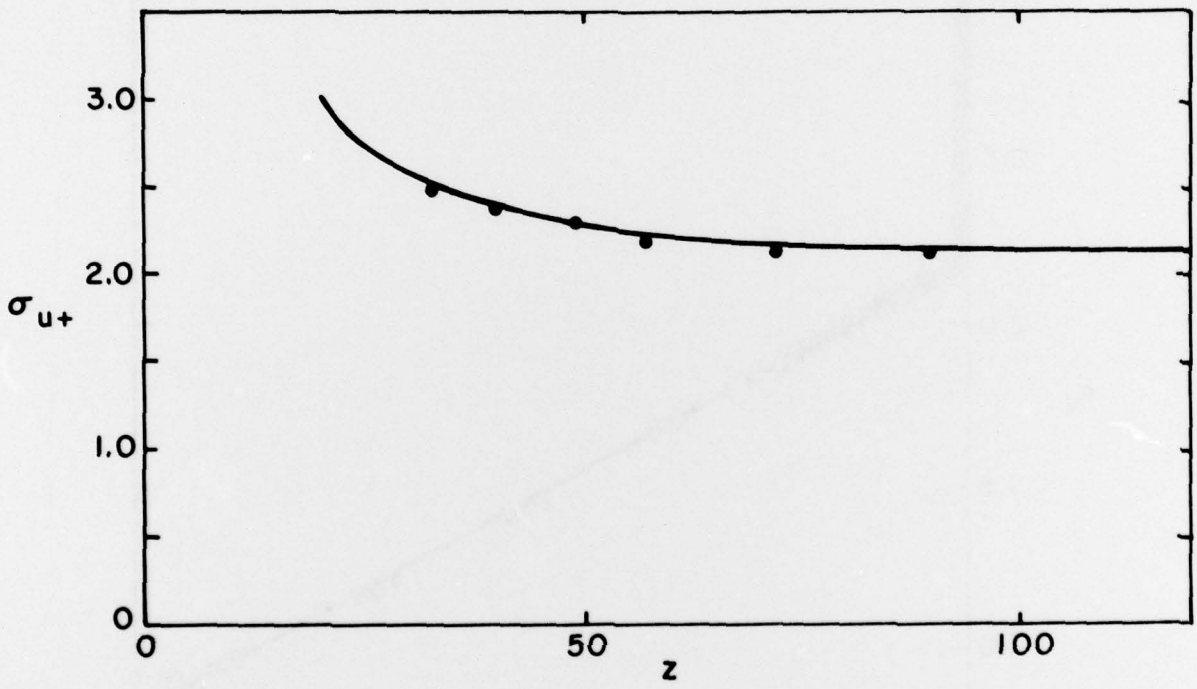
3.0
2.0
1.0
0
σ_{u+}
0
50
100
z

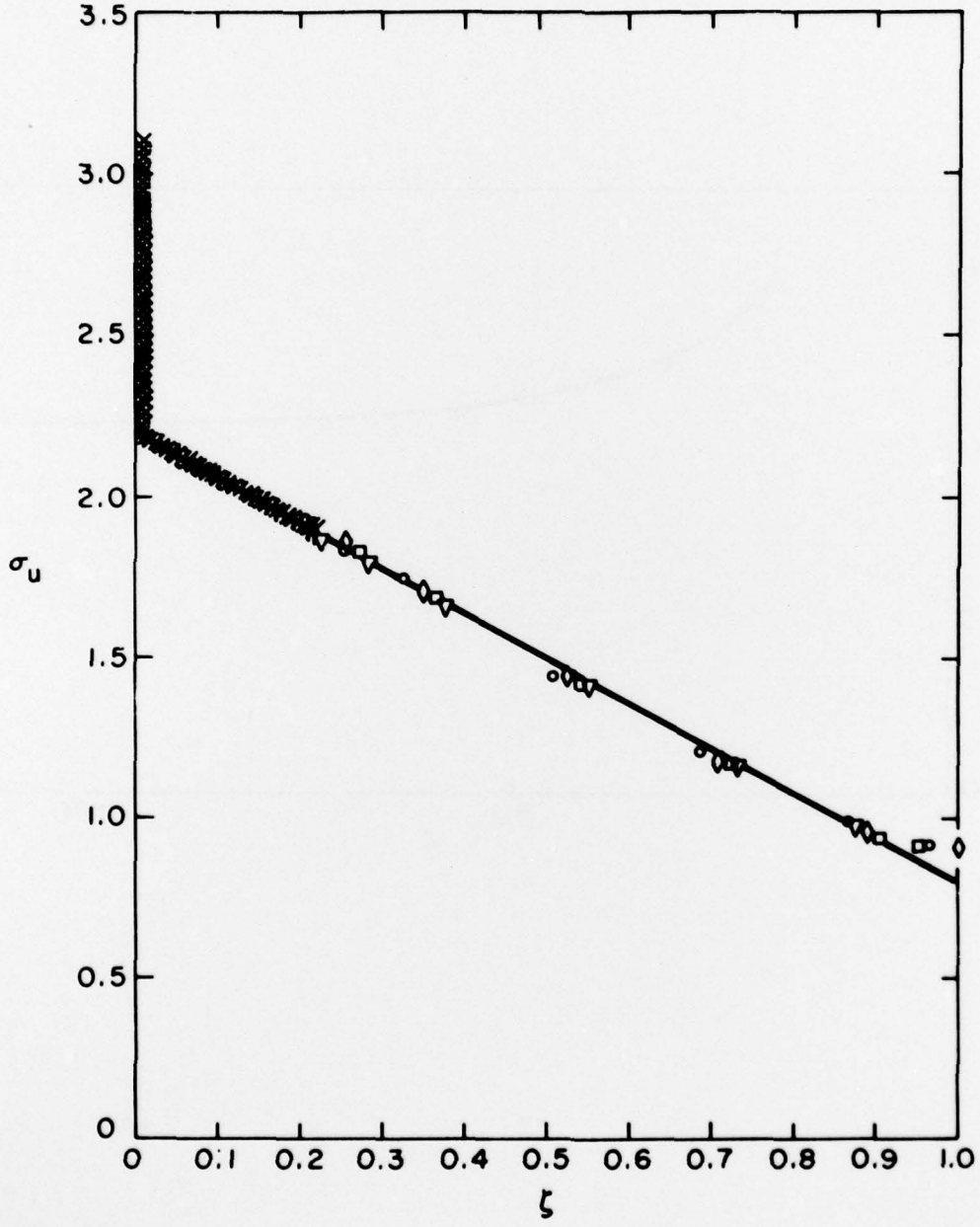
3.5
3.0
2.5
2.0
1.5
1.0
0.5
0
σ_u
0
0.1
0.2
0.3
0.4
0.5
0.6
0.7
0.8
0.9
1.0
ζ

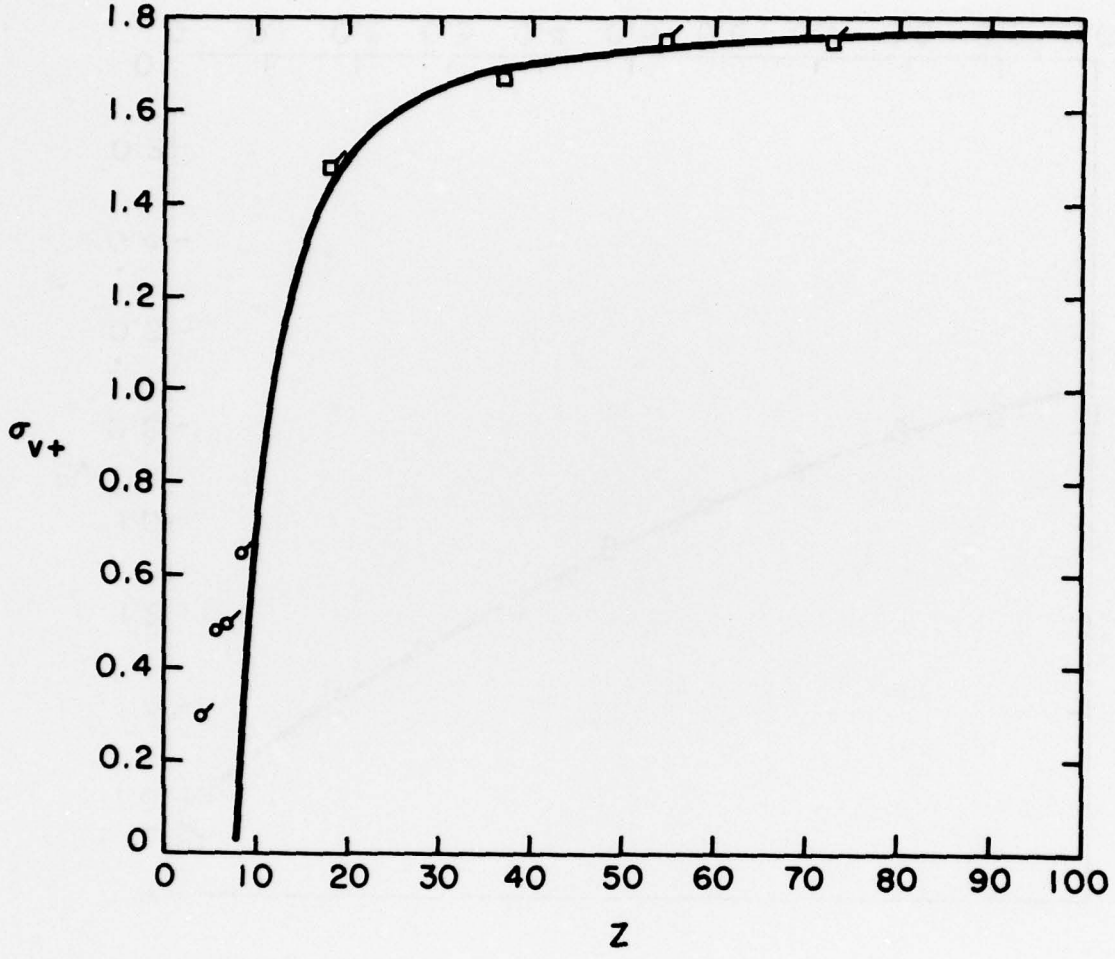
1.8
1.6
1.4
1.2
1.0
0.8
0.6
0.4
0.2
0
σ_{v+}
0
10
20
30
40
50
60
70
80
90
100
Z

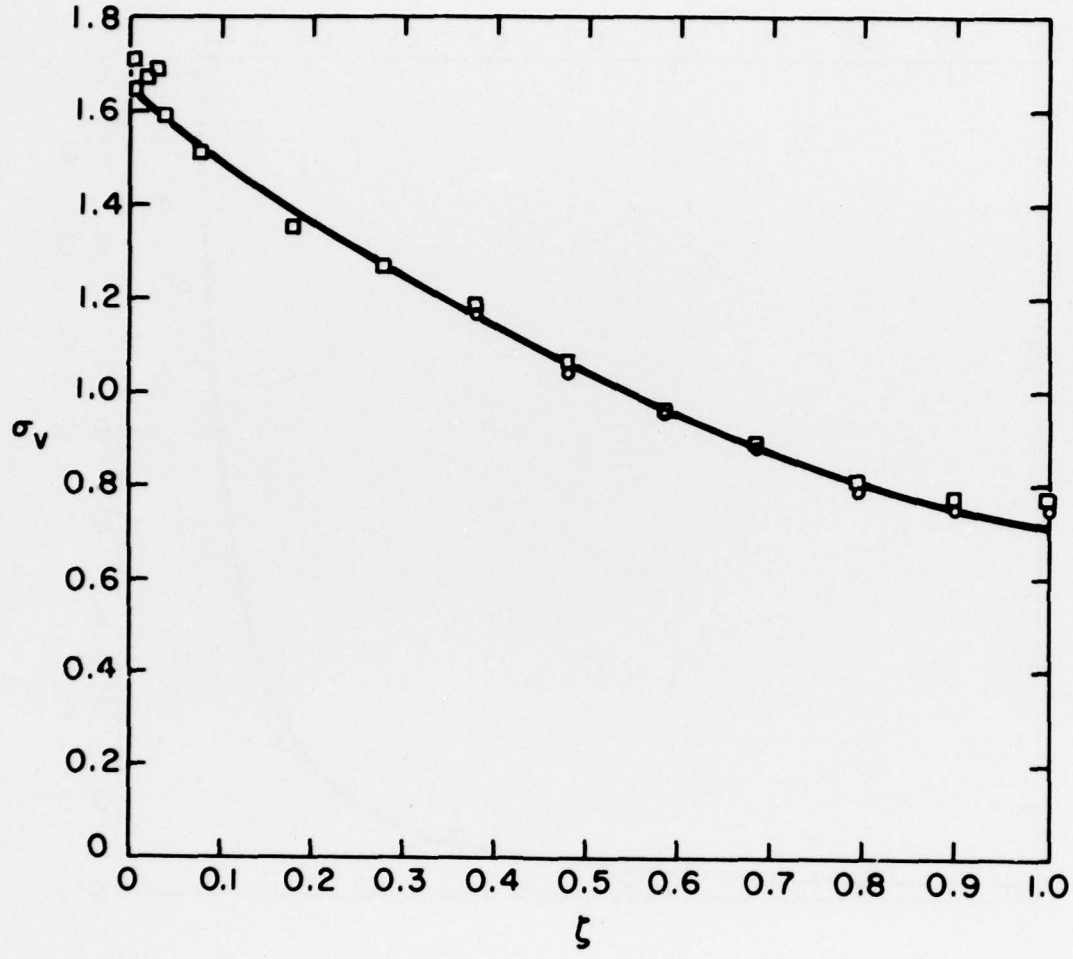
1.8
1.6
1.4
1.2
1.0
0.8
0.6
0.4
0.2
0
σ_v
0
0.1
0.2
0.3
0.4
0.5
0.6
0.7
0.8
0.9
1.0
ζ

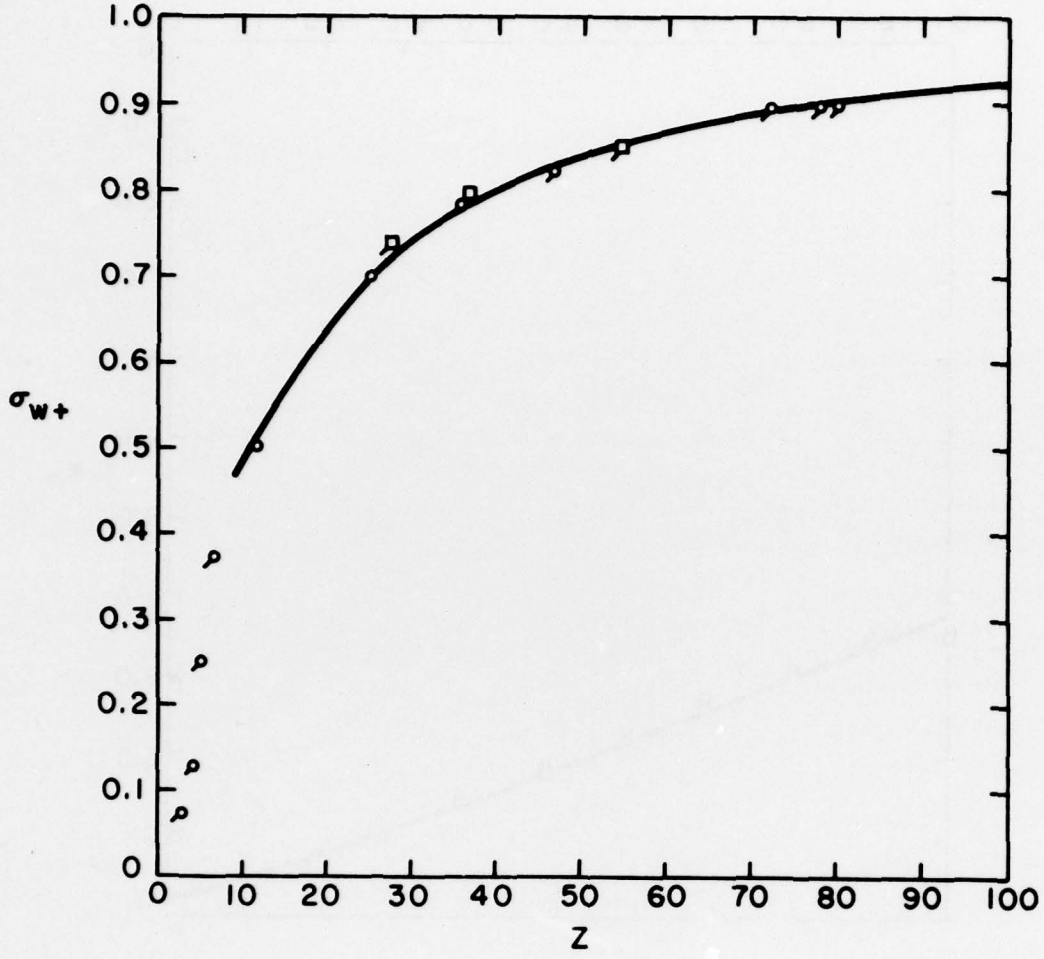
1.0
0.9
0.8
0.7
0.6
0.5
0.4
0.3
0.2
0.1
0
σ_{w+}
0
10
20
30
40
50
60
70
80
90
100
Z

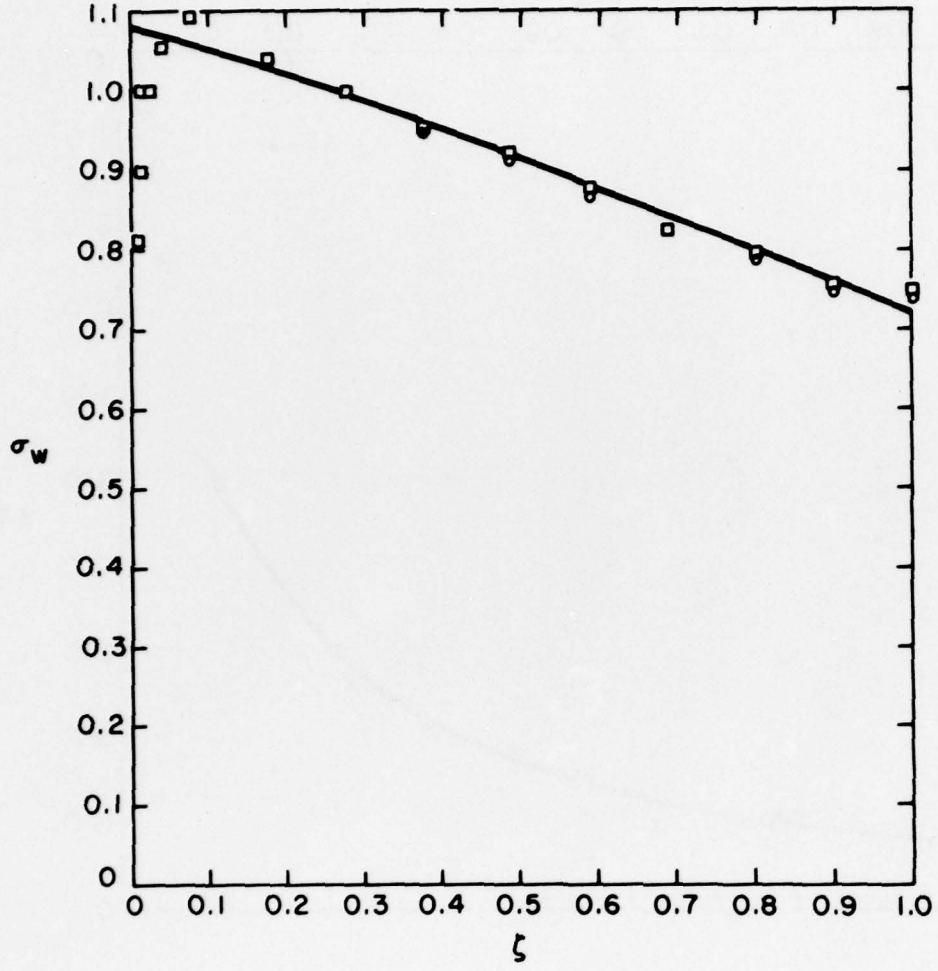
1.1
1.0
0.9
0.8
0.7
0.6
0.5
0.4
0.3
0.2
0.1
0
σ_w
0
0.1
0.2
0.3
0.4
0.5
0.6
0.7
0.8
0.9
1.0
ζ

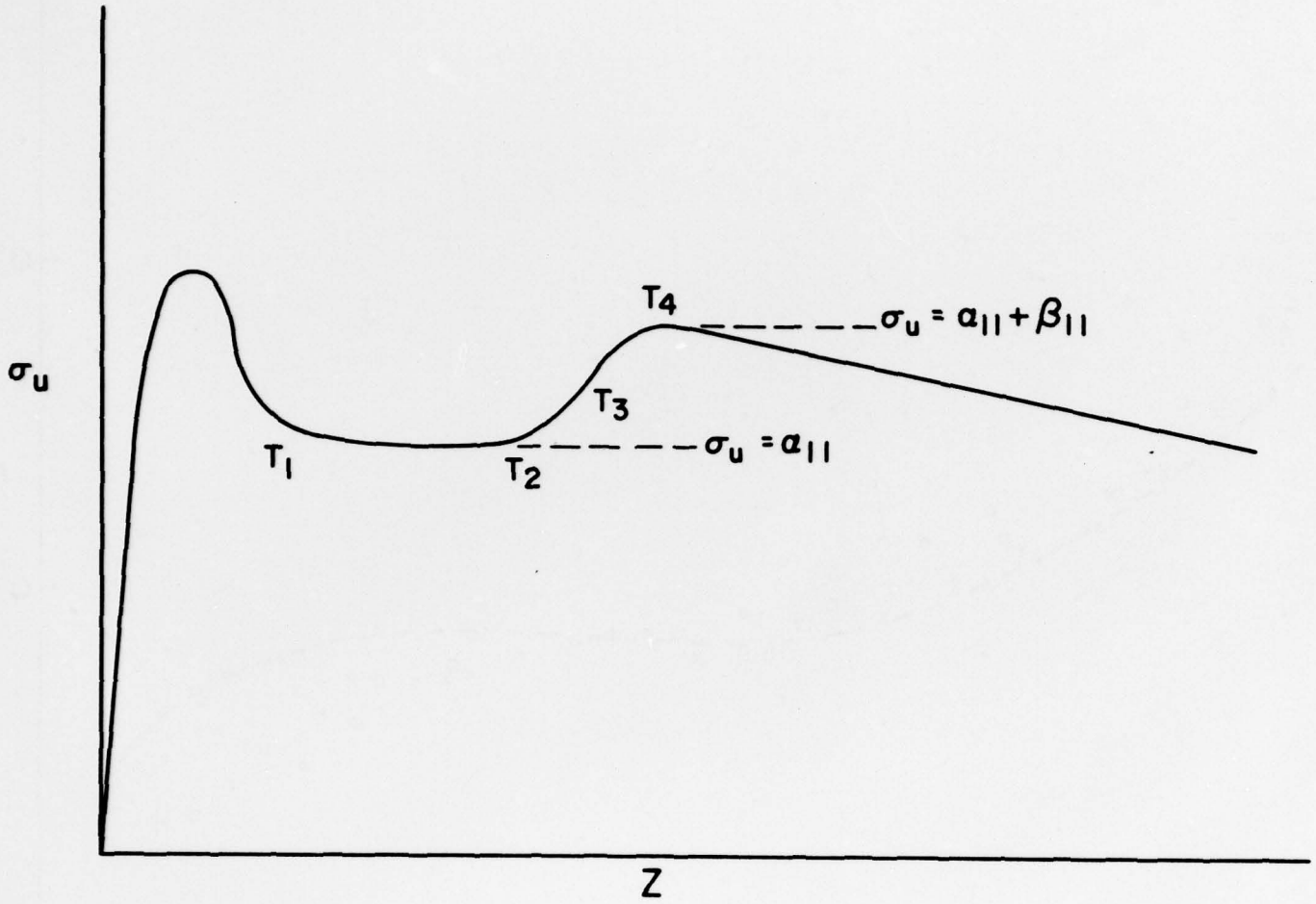
σ_u
T_4
$\sigma_u = \alpha_{11} + \beta_{11}$
T_3
T_1
T_2
$\sigma_u = \alpha_{11}$
Z

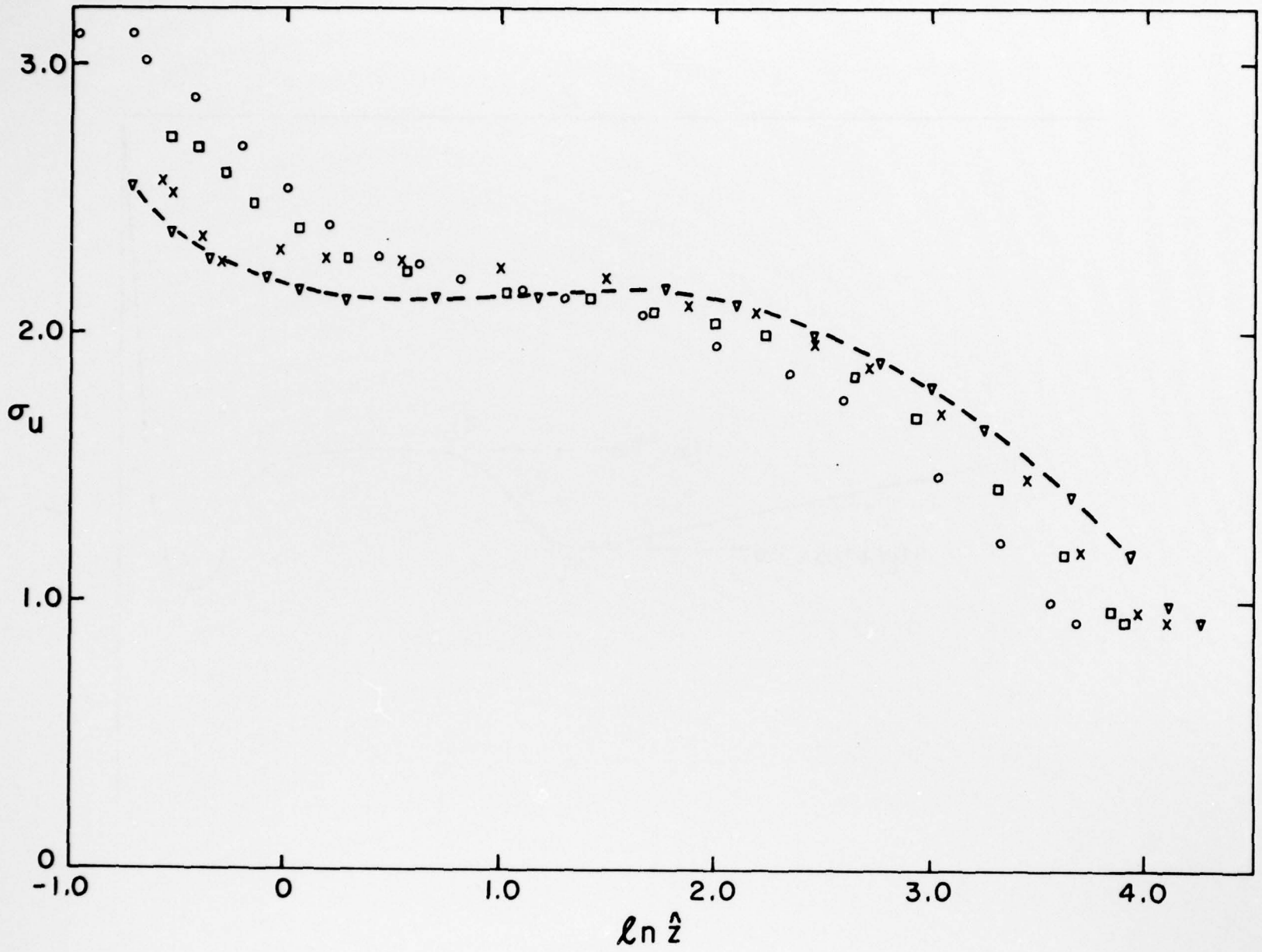
3.0
2.0
1.0
0
σ_u
-1.0
0
1.0
2.0
3.0
4.0
$\ell n \hat{z}$

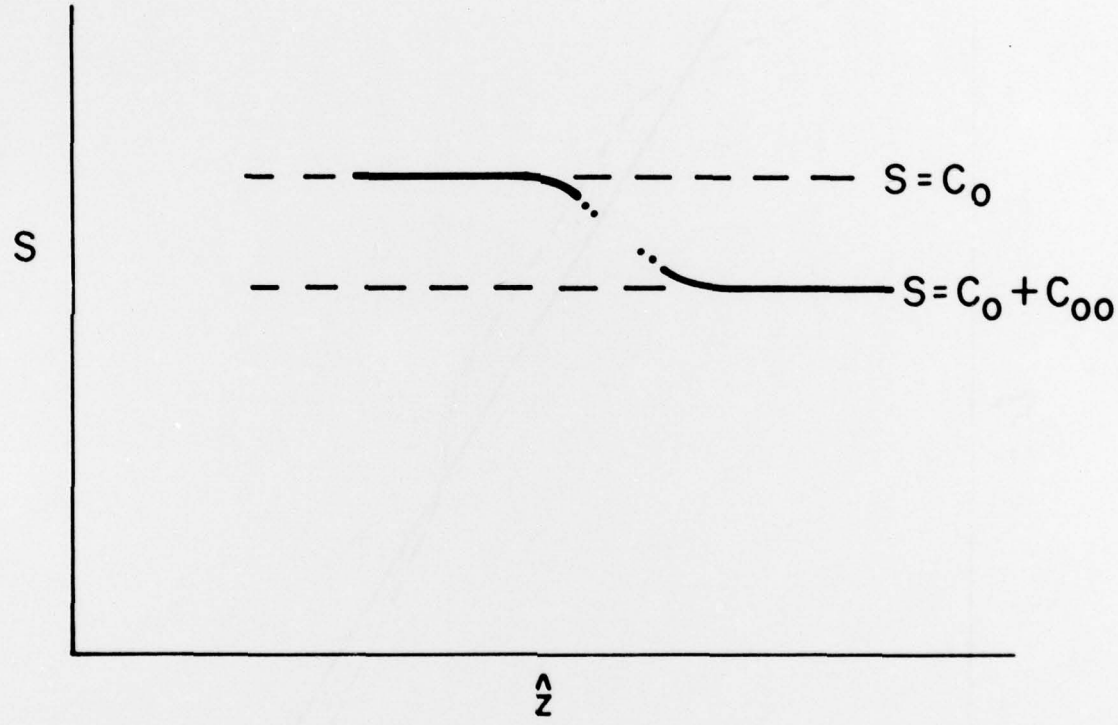
S
S = C_o
S = C_o + C_oo
ẑ

ln z
n

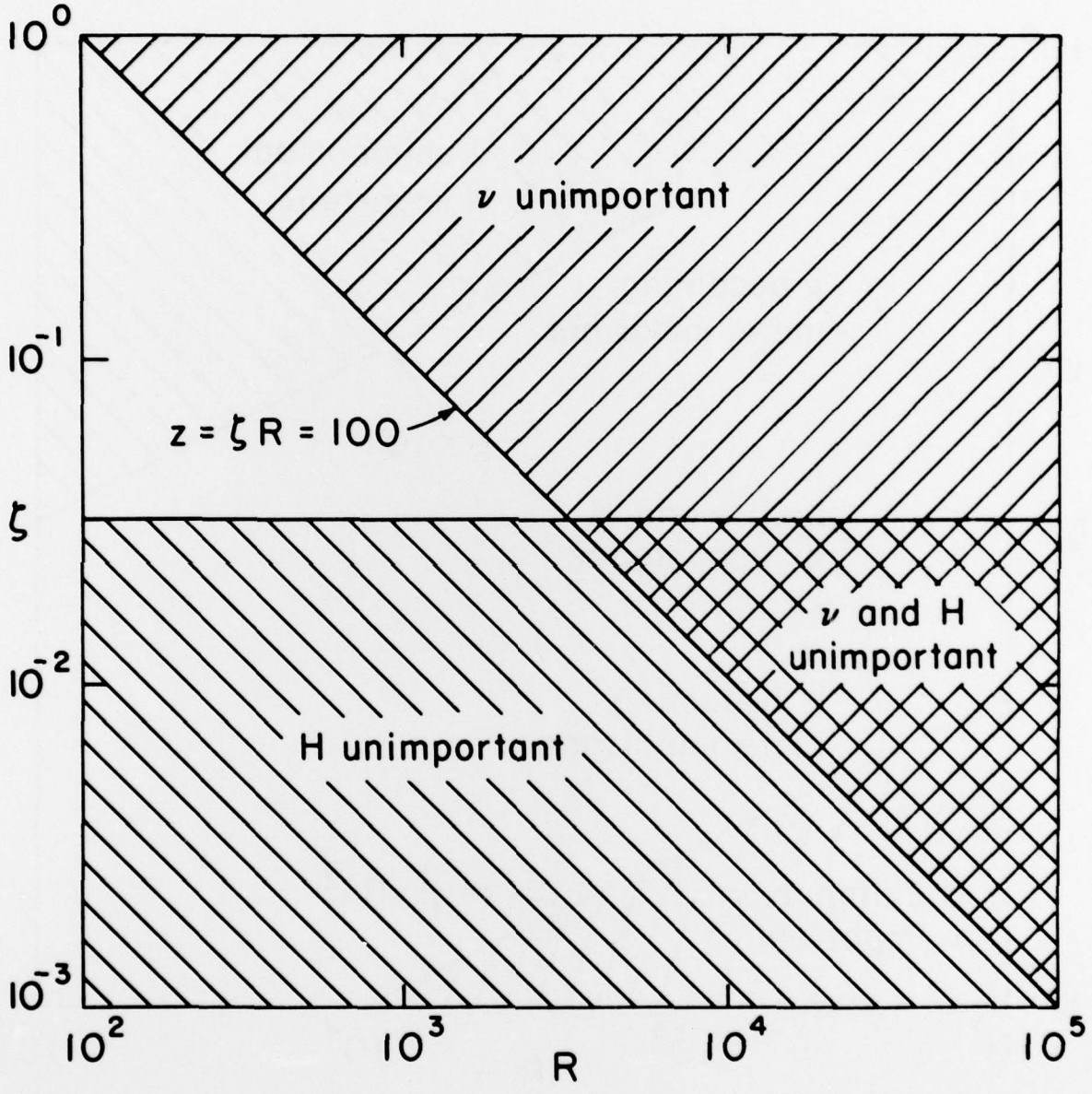
10^0
10^{-1}
10^{-2}
10^{-3}
ζ
ν unimportant
$z = \zeta R = 100$
ν and H unimportant
H unimportant
10^2
10^3
10^4
10^5
R

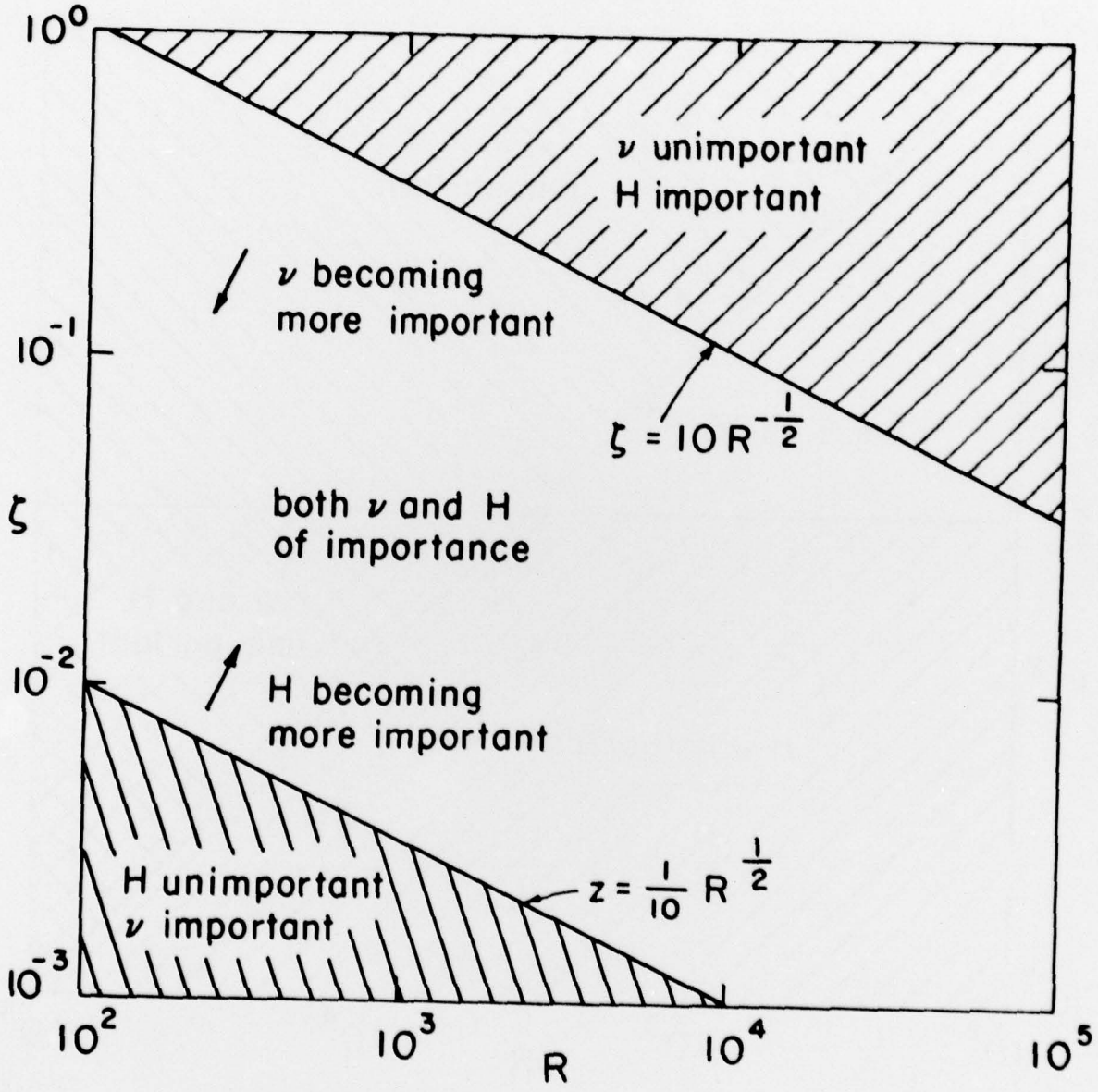
10^0
10^{-1}
10^{-2}
10^{-3}
ζ
ν unimportant
H important
ν becoming
more important
$\zeta = 10\,R^{-\frac{1}{2}}$
both ν and H
of importance
H becoming
more important
H unimportant
ν important
$z = \frac{1}{10}\,R^{\frac{1}{2}}$
10^2
10^3
10^4
10^5
R